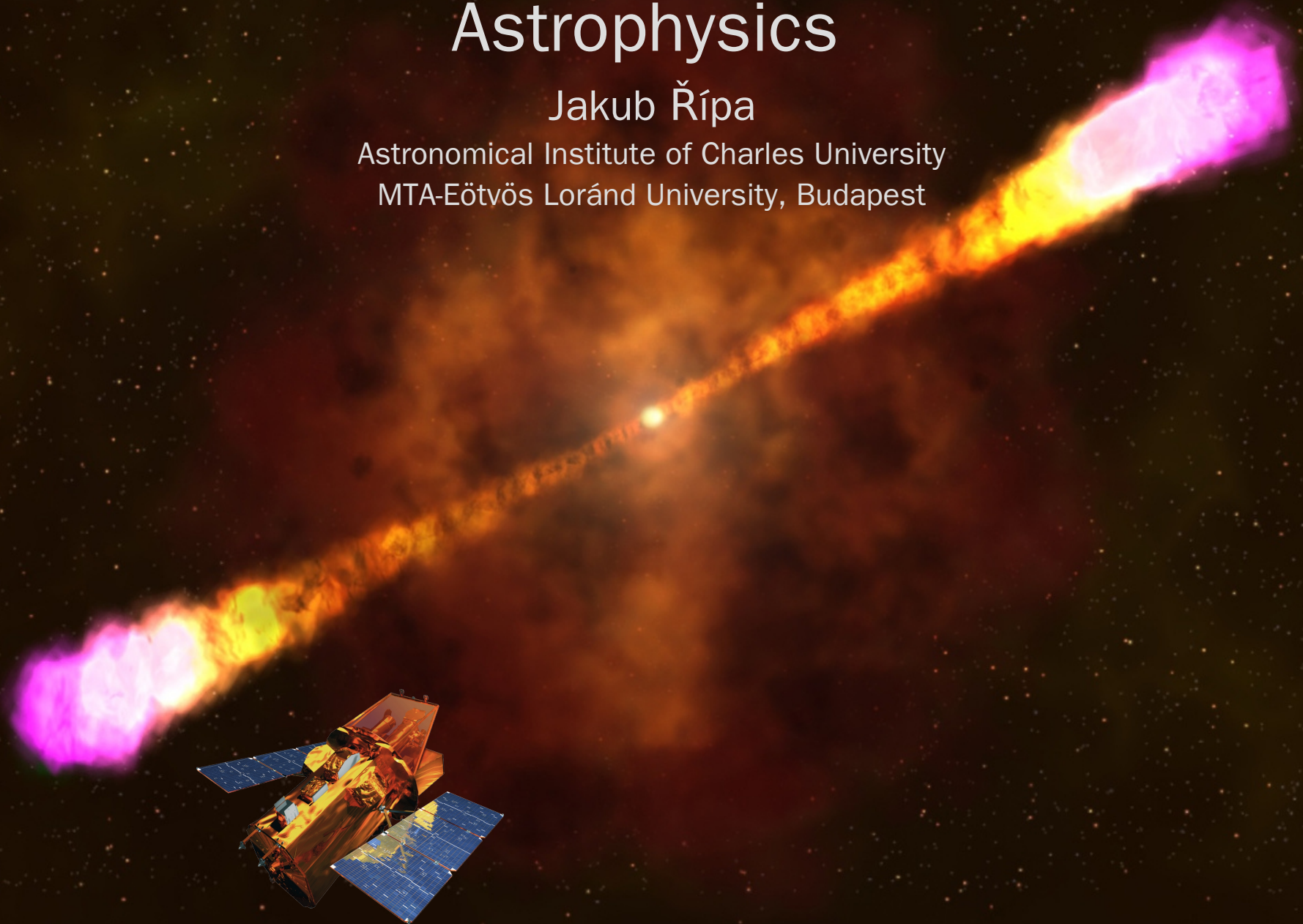


Introduction to Gamma-ray Burst Astrophysics

Jakub Řípa

Astronomical Institute of Charles University
MTA-Eötvös Loránd University, Budapest

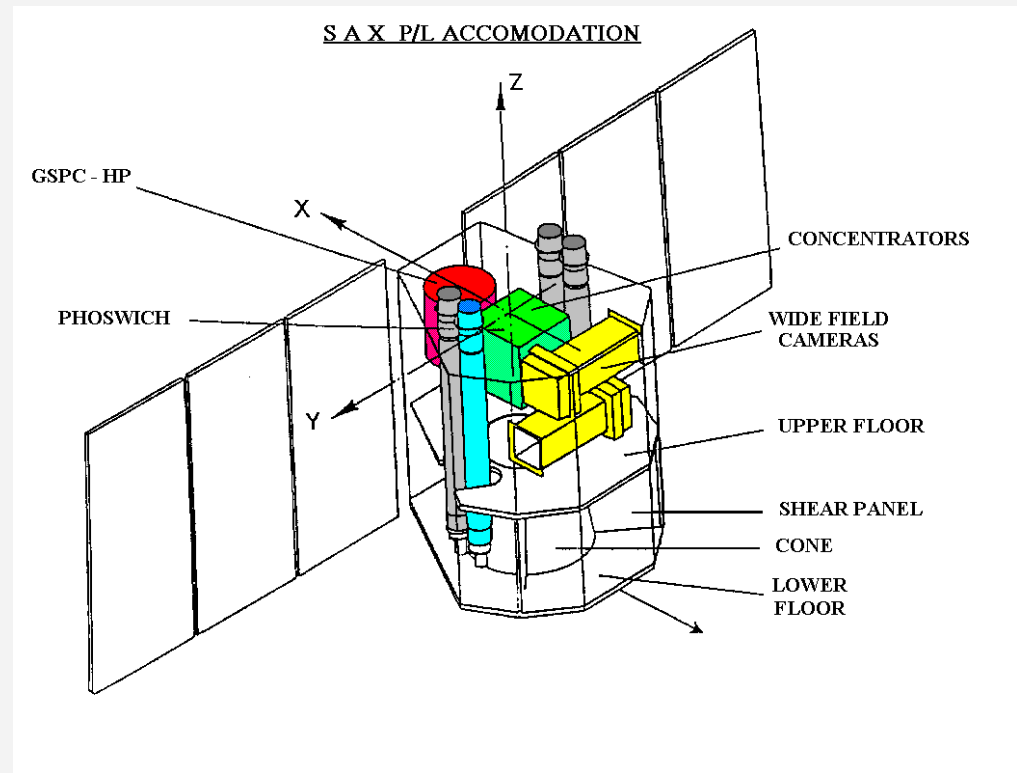


Afterglows

The *BeppoSAX* Breakthrough - Afterglow Era

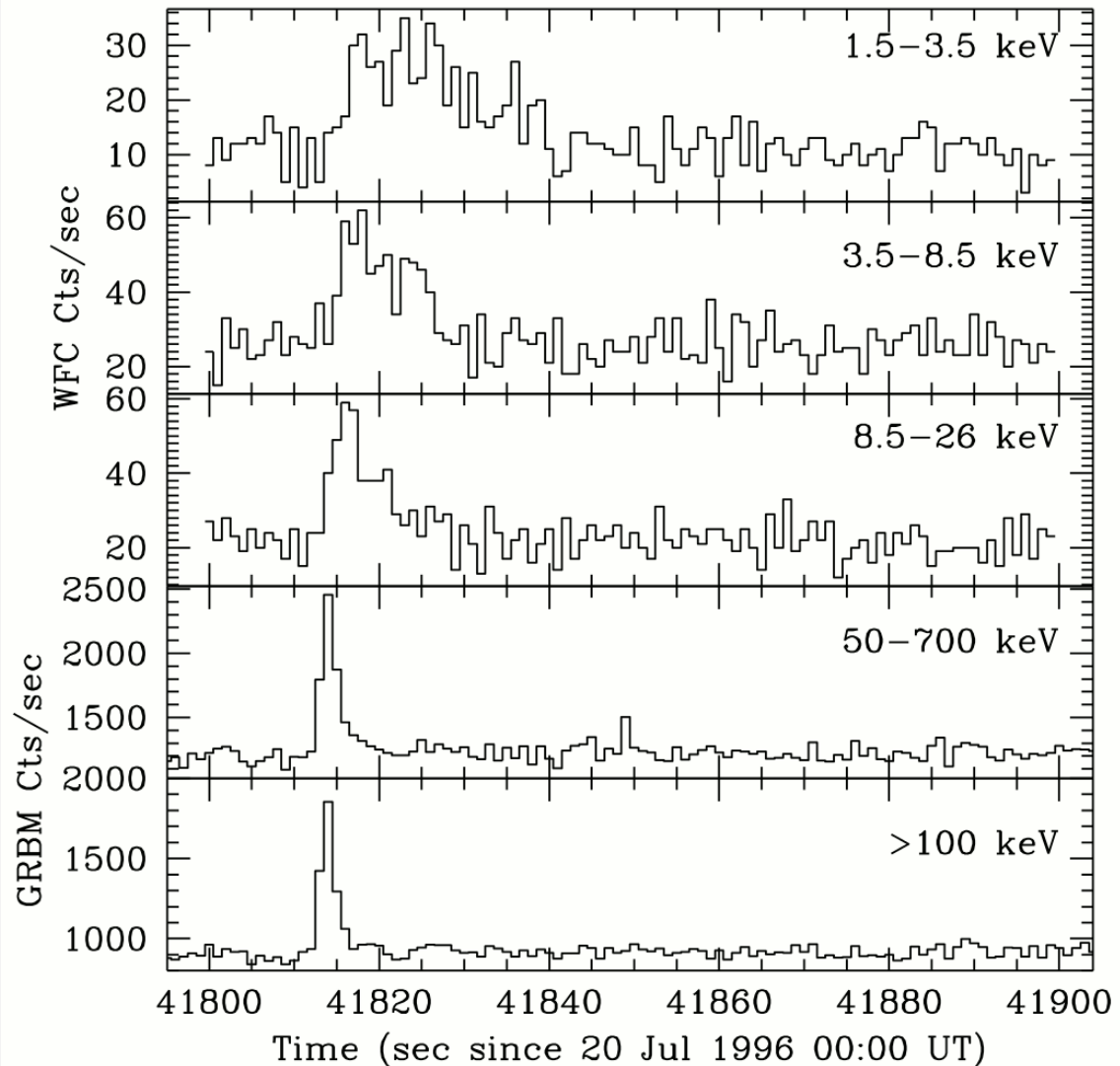


- Italian-Dutch satellite for X-ray astronomy (1996-2002)
- Wide energy range (from Gamma to soft X-rays: 0.1-700 keV)
- Good positional accuracy (~ 1 arcmin)
- Relatively fast repointing capabilities (down to 3-4 hours)



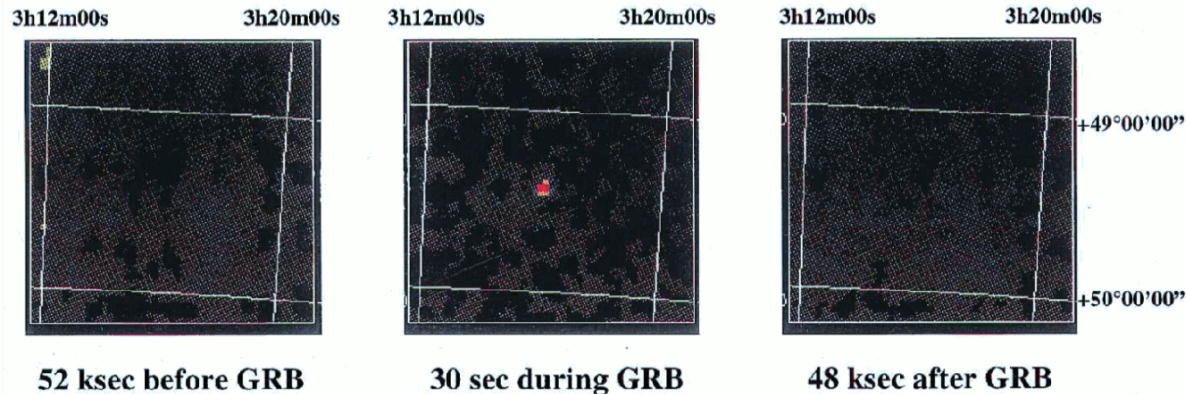
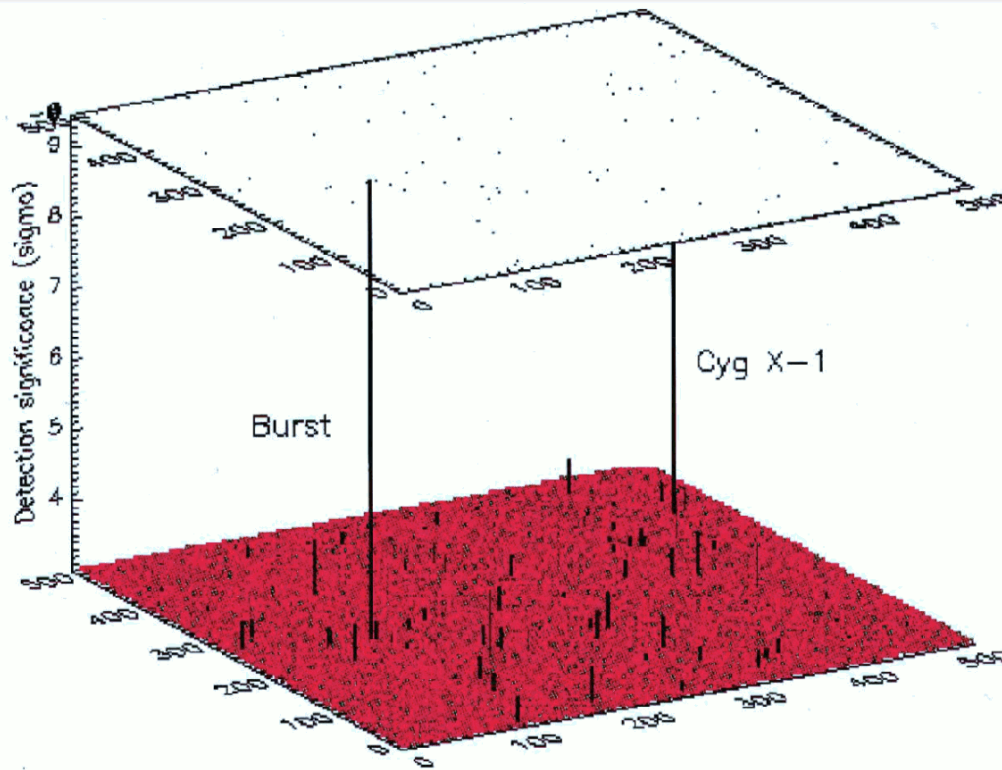
First X-ray localization of a GRB by *BeppoSAX*

- Fast and accurate localizations of gamma-ray bursts (GRB) by *BeppoSAX* allowed to establish the connection of GRB with the sources of decaying X-ray, optical, and radio emission.
- Simultaneous observation of GRBs by Gamma-Ray Burst Monitor and X-ray Wild-Field Camera.



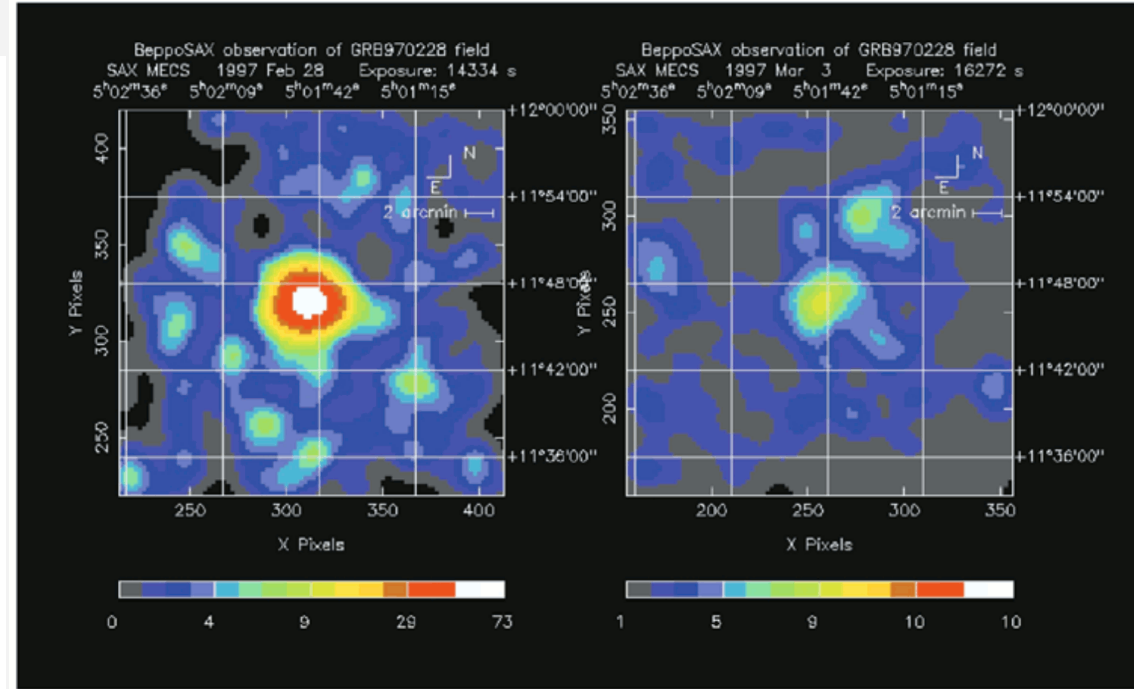
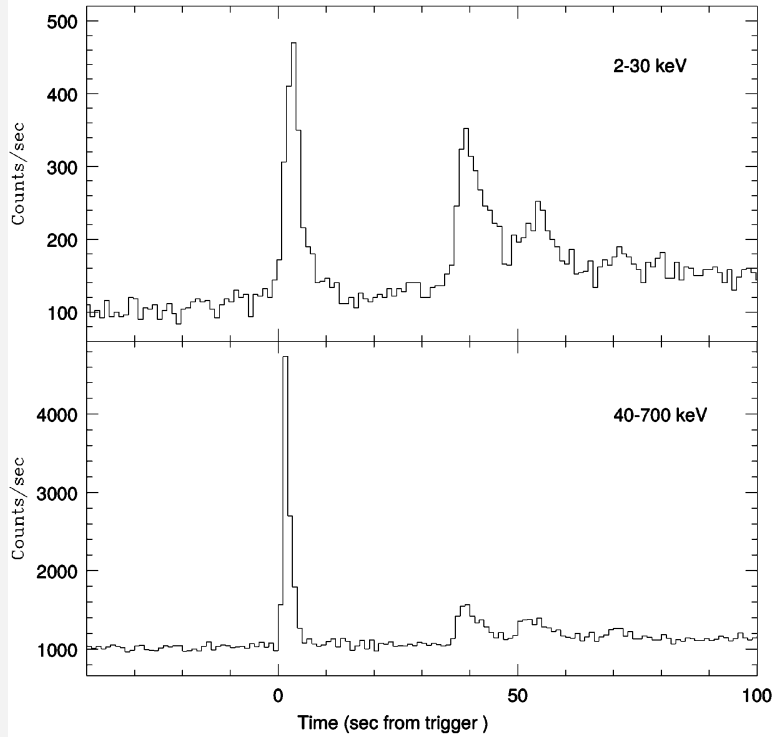
Light curves, by raw data, of the burst in four energy ranges: 2–8 keV, 8–26 keV (WFC); 50–700 keV, above 100 keV (GRBM).

First X-ray localization of a GRB by *BeppoSAX*



The $40^\circ \times 40^\circ$ image in the 2 – 26 keV range of the WFC integrated on a period of 15 s on the burst. The y axis gives the significance of the detection (σ). The source close to the edge is Cyg X-1. **b** Images of the field centered on GB960720 in time sequence. The first and last images were obtained integrating over $\sim 50,000$ s before and after the burst. No source was detected. The second image is a 30 s long shot which shows the sudden presence of GB960720. We find a 90% confidence level error circle for GB960720 that is centred on $\alpha(2000)=17^{\text{h}}30^{\text{m}}36^{\text{s}}$, $\delta(2000)=+49^\circ 05' 49''$ and has a radius of 3 arcmin. The position uncertainties have a statistical component depending on the source strength and a systematic component depending on the offset position in the field of view. Independent checks of the images scales, and a modelling of the spectrally and positionally dependent point spread function have been performed. The distribution of the error was checked with 93 independent sources.

GRB 970228

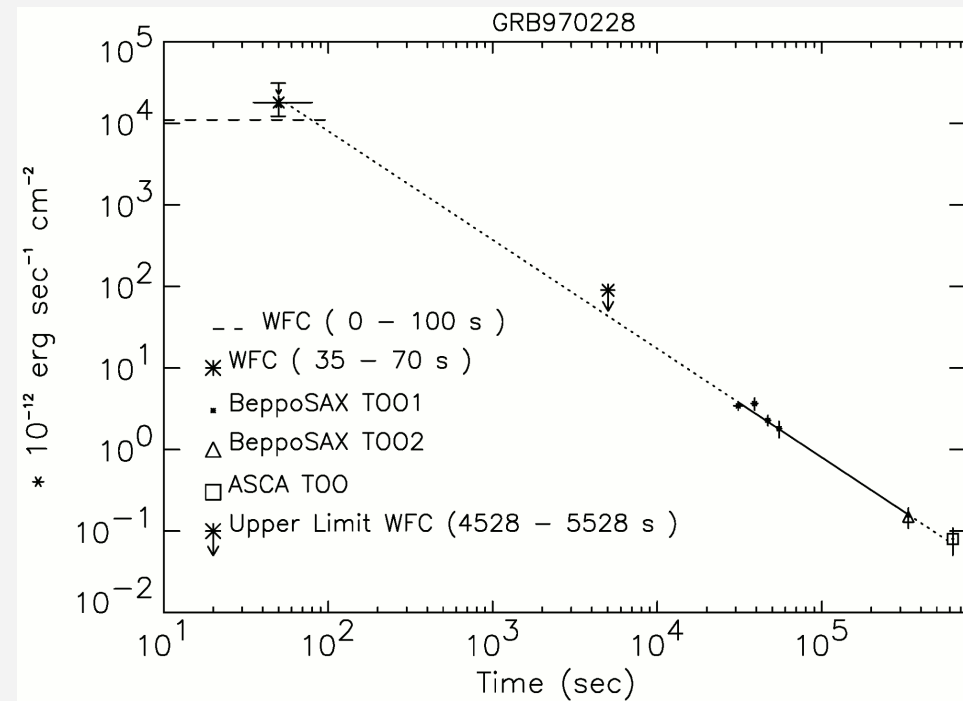


Images of the source 1 SAX J0501.7+1146, detected with the BeppoSAX Medium Energy Concentrator Spectrometer (2–10 keV) in the error box of GRB970228, during two target of opportunity (TOO) observations. The first observation started only 8 h after the GRBM trigger. The second observation was performed about three days after the GRB. The source faded by a factor of ~ 20 in 3 days (Costa et al. 1997e).

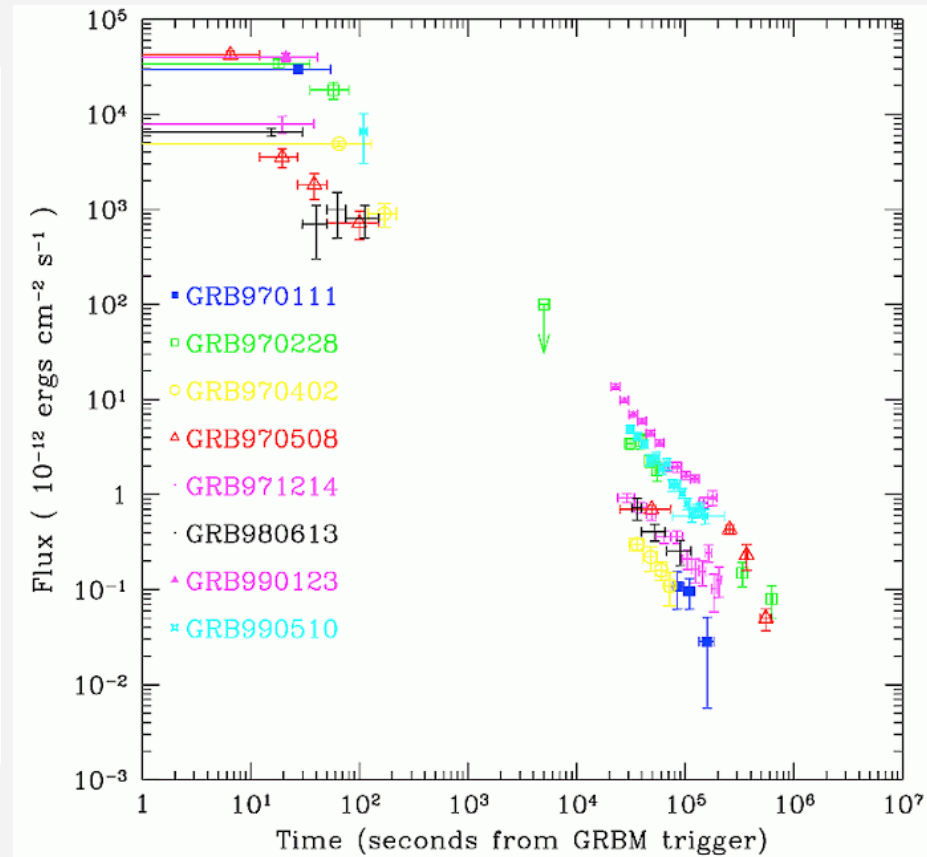
Long-duration GRB

Costa et al. 1997

BeppoSAX X-Ray Afterglows

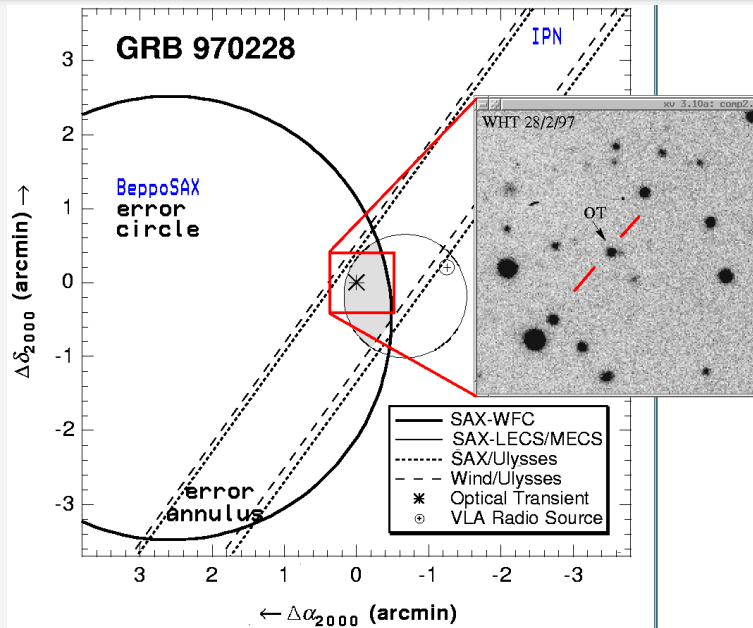


Variation with time of the X-ray flux from GRB 970228, in the 2-10 keV energy range (Costa et al. 1997).

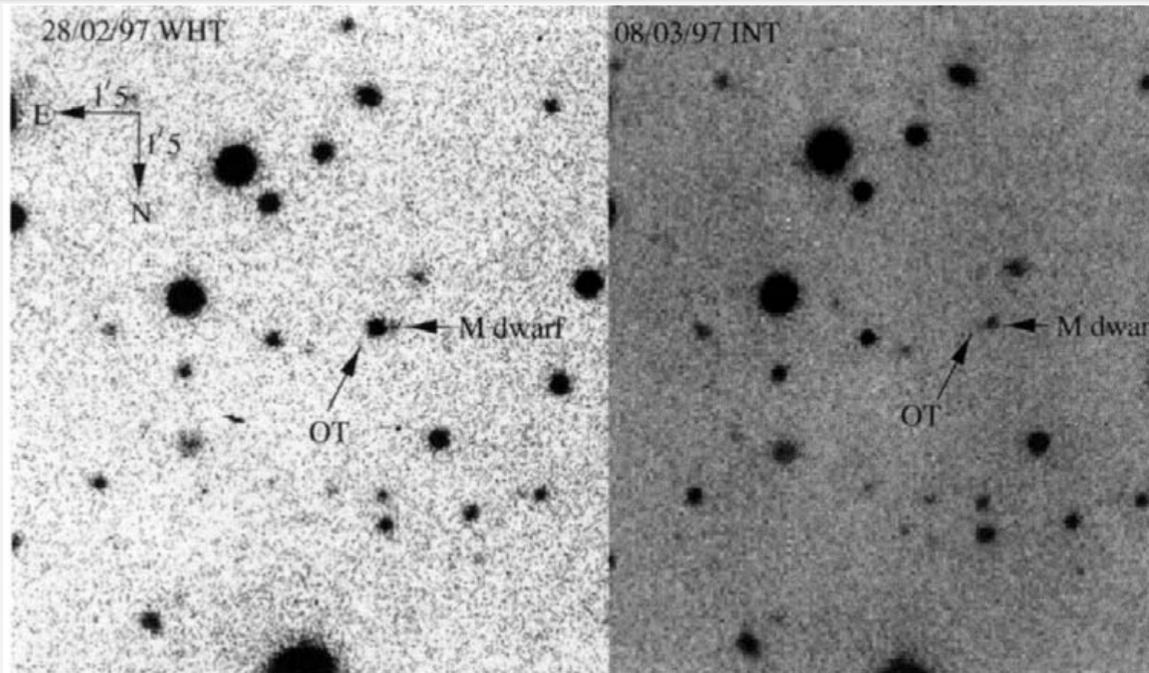
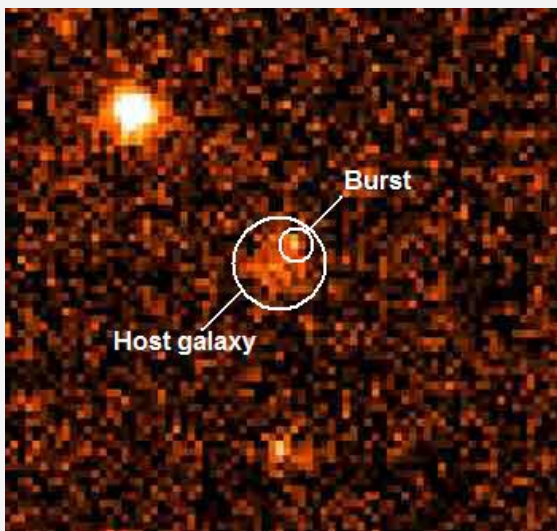


X-ray fading source
Power-law decay: $F \propto t^{-1.3}$

BeppoSAX GRB 970228 - First Optical Counterpart



Fading optical source within the *BeppoSAX* NFI error circle.

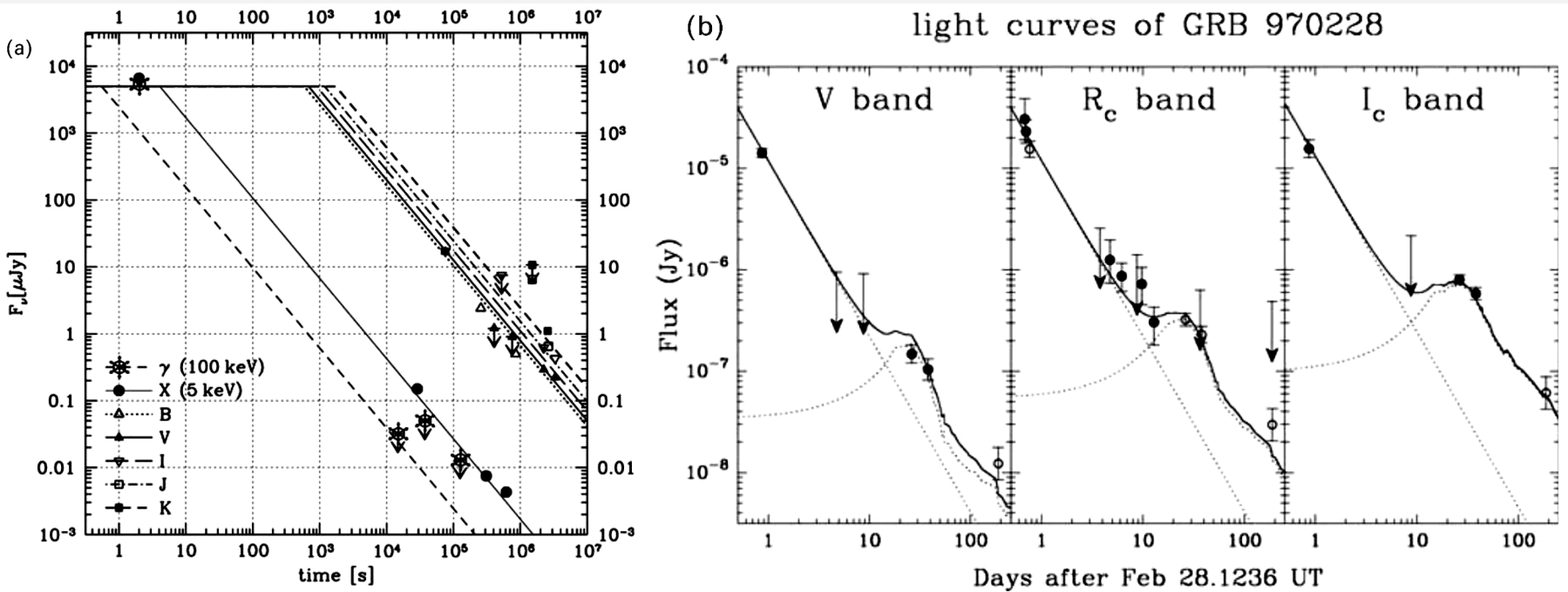


V-band images of a $1.5' \times 1.5'$ region of the sky which contains the optical transient (OT) associated with GRB 970228. The leftmost image was obtained with the William Herschel Telescope on La Palma on February 28, 1997, at 23:48 UT, less than 21 h after the burst (Groot et al. 1997a,b). The rightmost image was obtained with the Isaac Newton Telescope on March 8, at 20:42 UT. A large brightness variation is seen between the two images. An M dwarf star separated from the optical transient by $2.9''$ is also indicated (van Paradijs et al. 1997).

van Paradijs et al. 1997

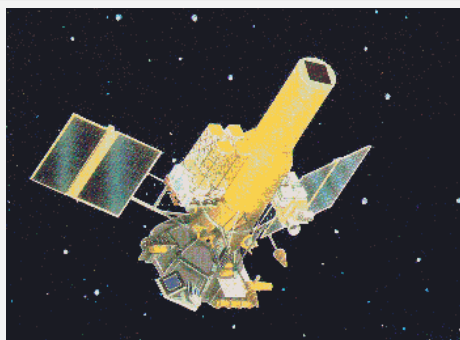
- Found to lie near a faint and distant galaxy of redshift $z = 0.695$ (luminosity distance $D_L = 4.27$ Gpc).
- Cosmological distance confirmed !
- First measured redshift of short-duration ($T_{90}=70$ ms) GRB 050509B at $z = 0.225$.

GRB 970228 - From Near-Infrared to X-ray Afterglow and SN Connection



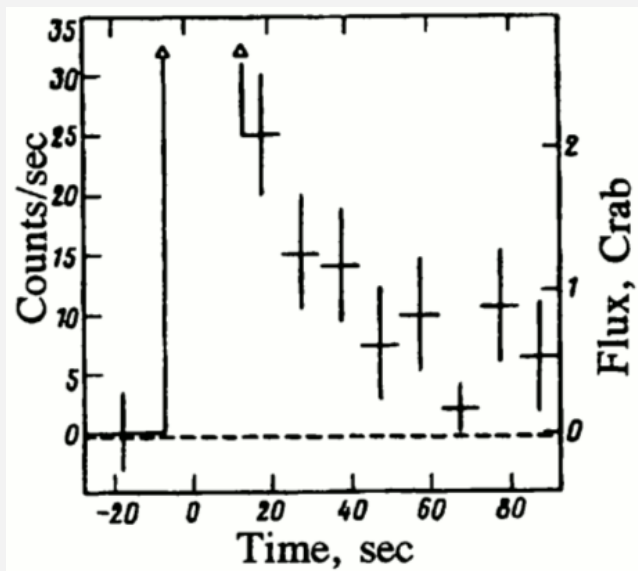
(a) Light-curves of the afterglow of GRB 970228 at various wavelengths, from X-rays to near-infrared. The lines indicate a quite convincing comparison with the predictions of the simplest external shock scenario (Wijers, Rees, & Meszaros 1997). (b) The afterglow of GRB 970228 measured in the V, R_c , and I_c bands at late times (beyond 1 day; Galama et al. 2000—Figure 3.3). The light-curves present a bump that has been interpreted as the contribution from an underlying supernova (Reichart 1999, Galama et al. 2000). The afterglow is modeled with a power-law decay ($F \propto t^{-1.51}$) plus the contribution of a supernova like SN 1998bw, redshifted at $z = 0.695$, the redshift of GRB970228 (Djorgovski et al. 1999).

First X-Ray/Gamma-Ray Afterglow Before *BeppoSAX* ?

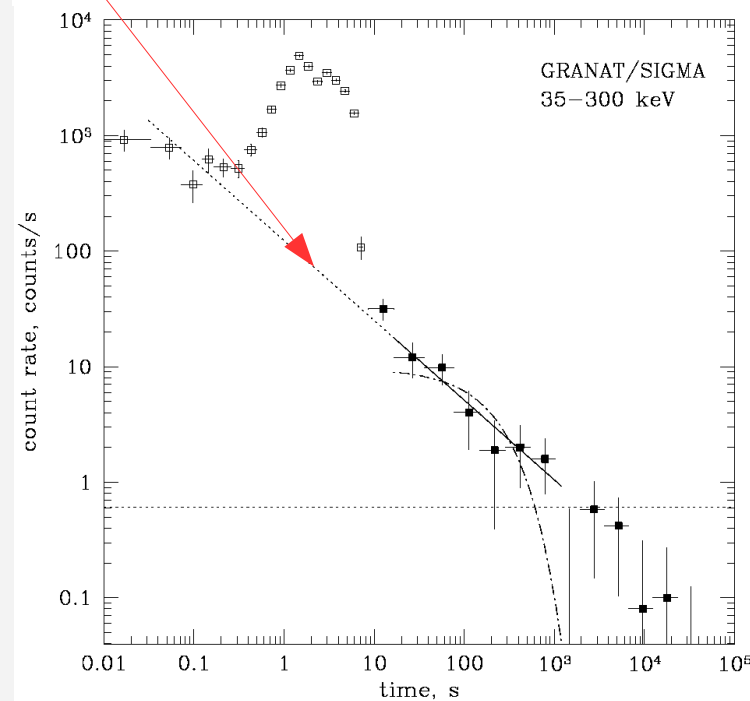
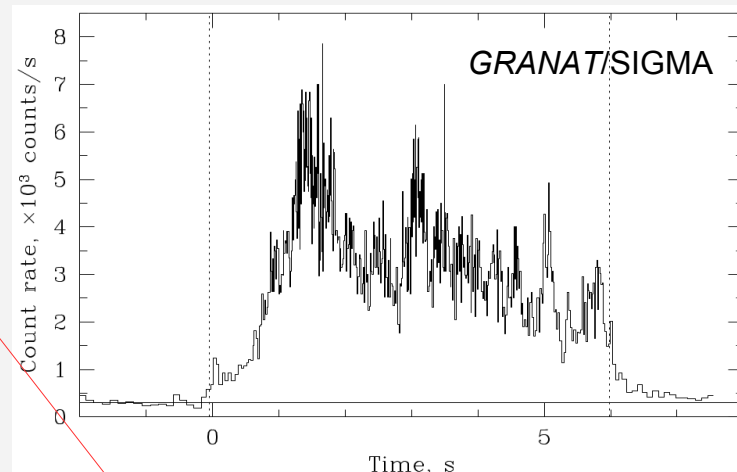


GRANAT

- GRB 920723B: the first X-ray afterglow?
- Flux decaying as power-law $\sim t^{-0.7}$



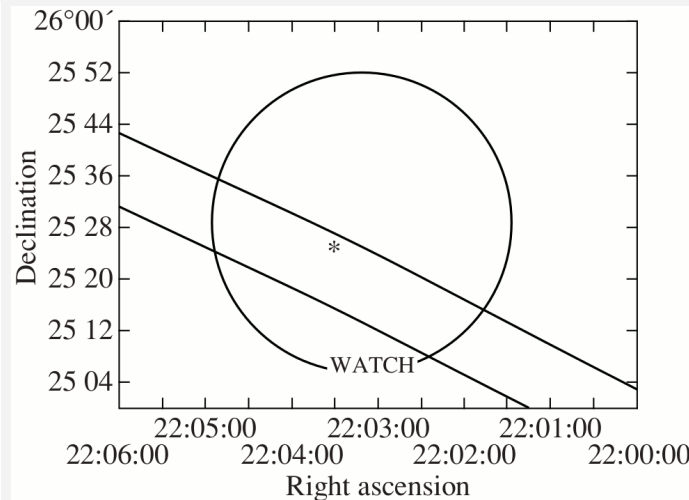
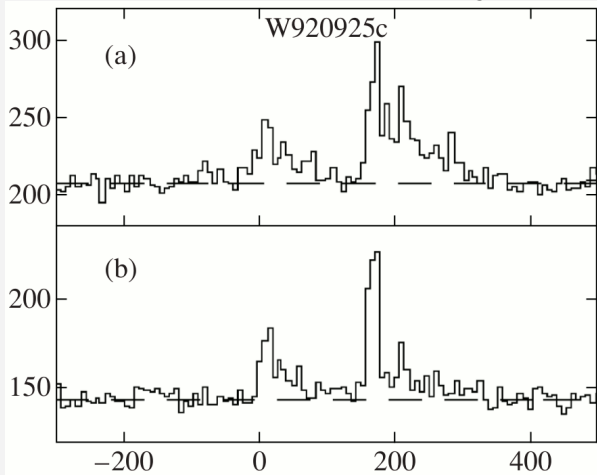
- GRANAT/WATCH
8-20 keV after end of GRB 920723B
(Therekov et al. 1993)



Burenin et al. (1999)

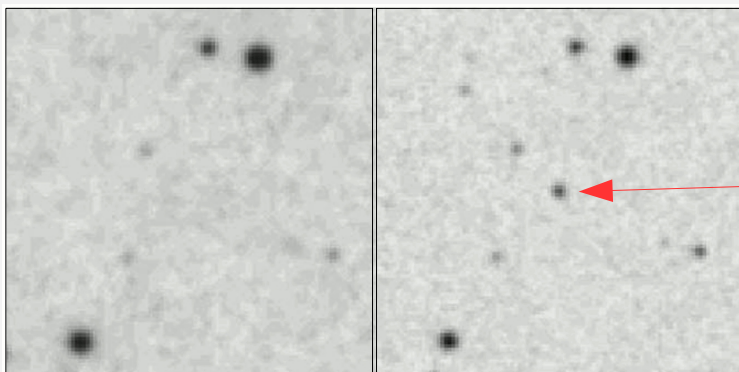
First Optical Afterglow Before *BeppoSAX* ?

- Archival images for the error boxes of GRBs obtained at the Palomar (USA) and Siding Spring (Australia) Observatories during the DSS all-sky survey has revealed an optical transient with a magnitude of 17.8 within the error circle of the bright event GRB 920925C (observed by *GRANAT* / *WATCH*, *GRANAT* / *PHEBUS* and *Ulysses*) on the plate taken 6-7 h after the burst. The position of the object falls within the IPN error box for the burst.



WATCH (circle) and IPN (band) error boxes for GRB 920925C; the asterisk marks the position of the optical transient.

Denisenko and Terekhov (2007)

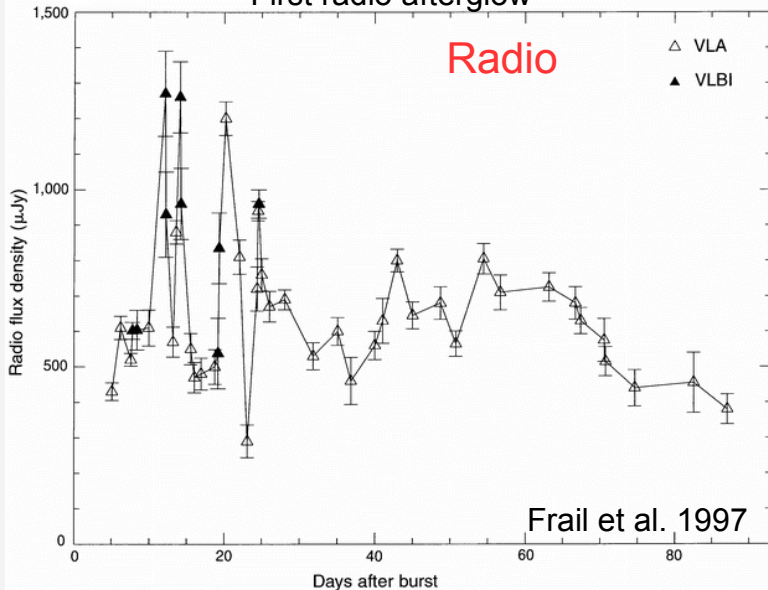


Images of the optical afterglow region on the blue Palomar 1950 (left) and 1992 (right) plates.

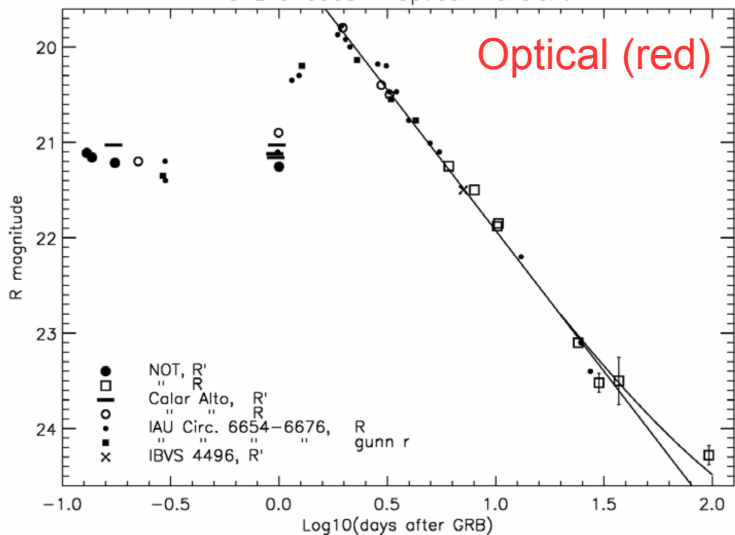
- GRB 920925C: the first optical afterglow?
- $B = 17.8 \pm 0.1m$, 6-7 h after the burst.

GRB 970508 - Afterglow from X-ray to Radio

First radio afterglow



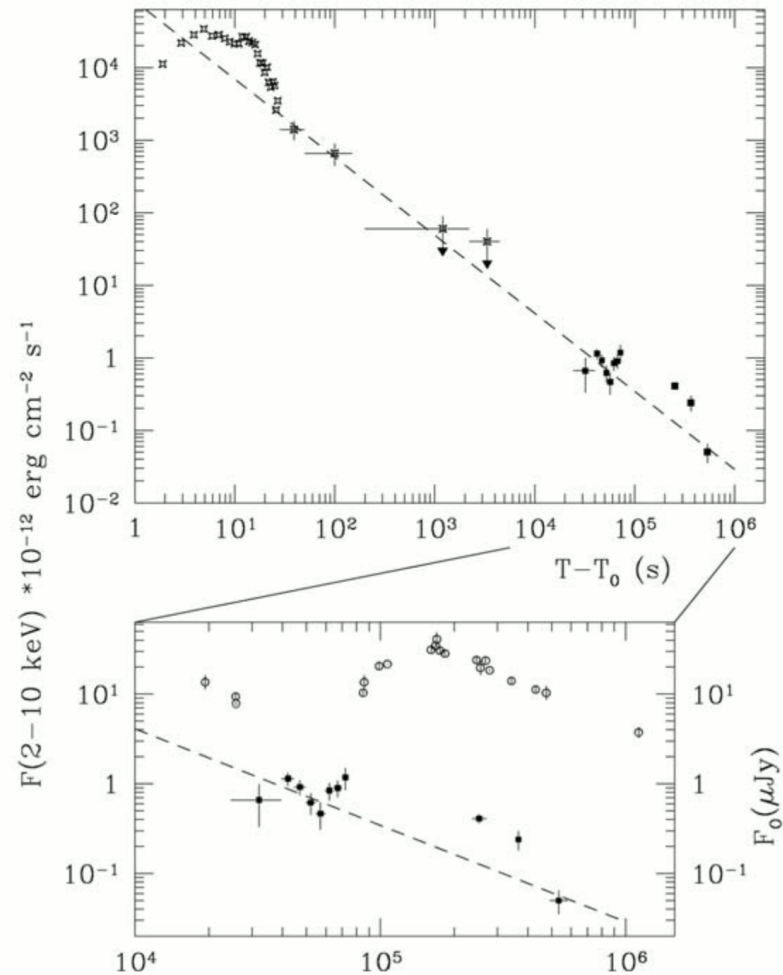
GRB 970508 - Optical Transient



R-band light-curve of the optical transient associated with GRB 970508. Following a period of modest decline, a peak of optical emission was reached about 40 h after the GRB. After this peak, the emission declines following a power law ($F \propto t^{-1.21}$). A possible contribution of a constant source, the host galaxy with R -magnitude of 25.5 is shown by the curved line at the lower right of the figure (from Pedersen et al. 1998; see also Figure 3 of Fruchter et al. 2000b).

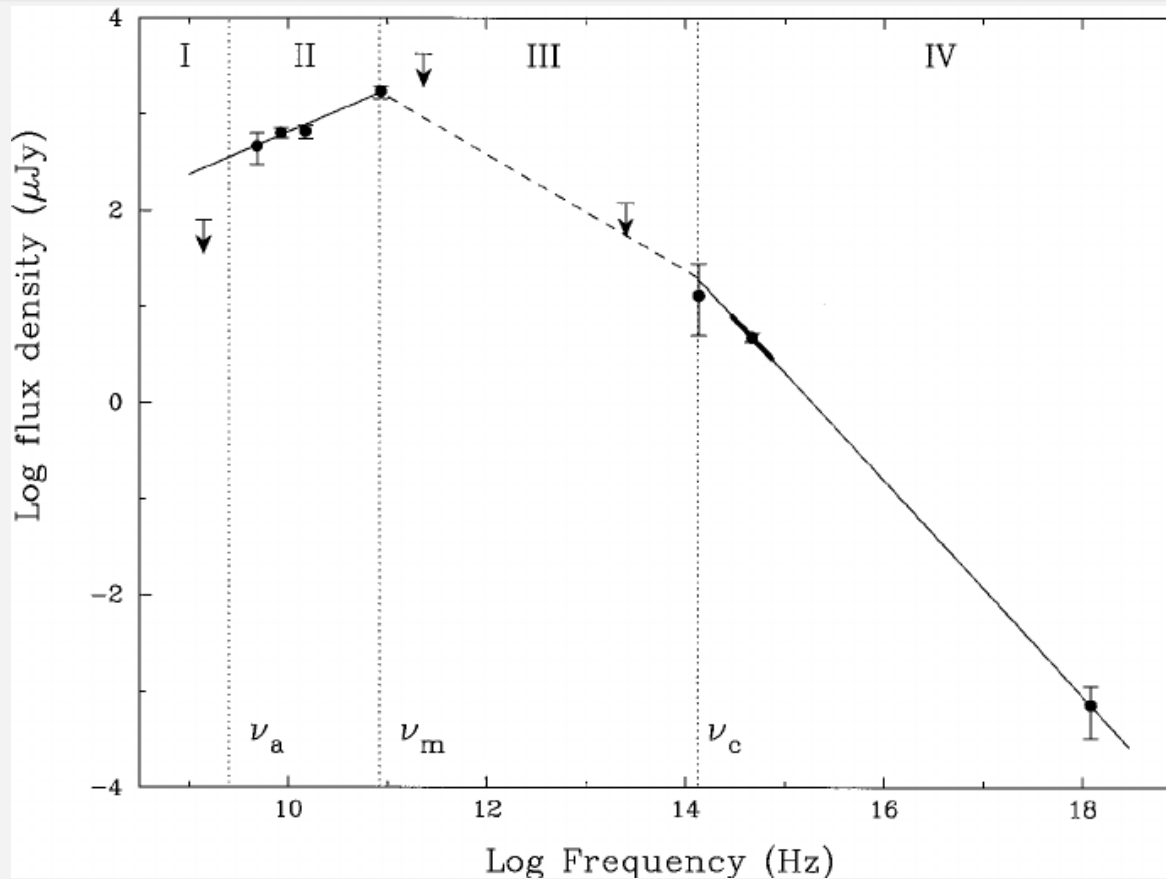
X-rays

X-ray light-curve (2–10 keV) of GRB 970508 and its afterglow (WFC and NFI). The dashed line shows the best-fit power law. The lower panel displays the behavior of the source in the optical R band, from 10^4 to 10^6 s (see also Figure 3.5), clearly showing a late time (~ 1 day) outburst that is concomitant with a bump in the X-ray light-curve (from Piro et al. 1998a).



- The damping of the fluctuations in the radio afterglow indicated the increase of the size of the radio emitter and that radio-emitting region expanded with a velocity very close to the speed of light (Frail et al. 1997). This result supported the relativistic fireball model of GRBs (more later).

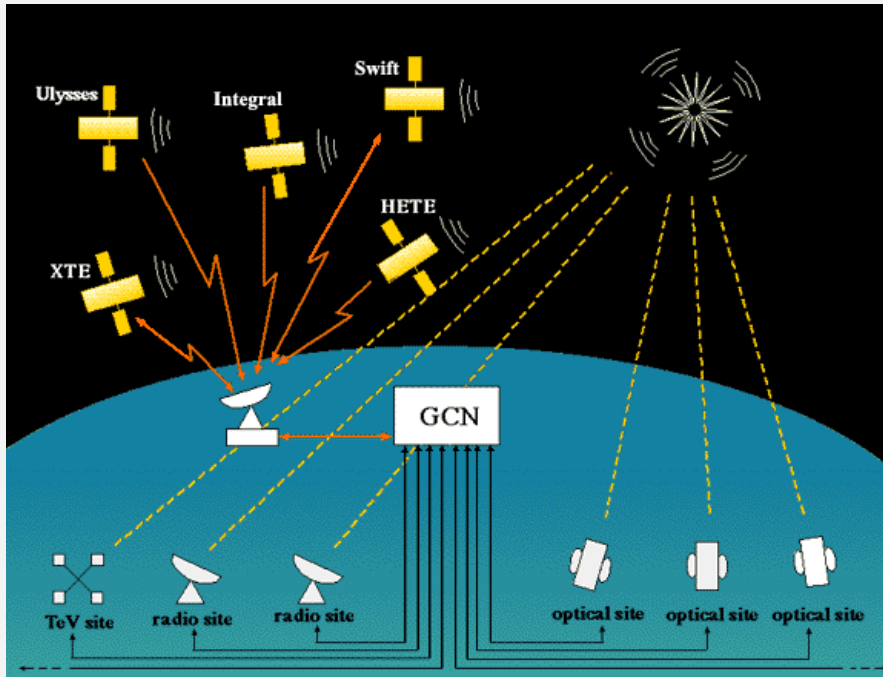
GRB 970508 - Spectrum of Afterglow from X-ray to Radio



The radio to X-ray energy spectrum of GRB 970508 as measured 12.1 days after the burst (Galama et al. 1998).

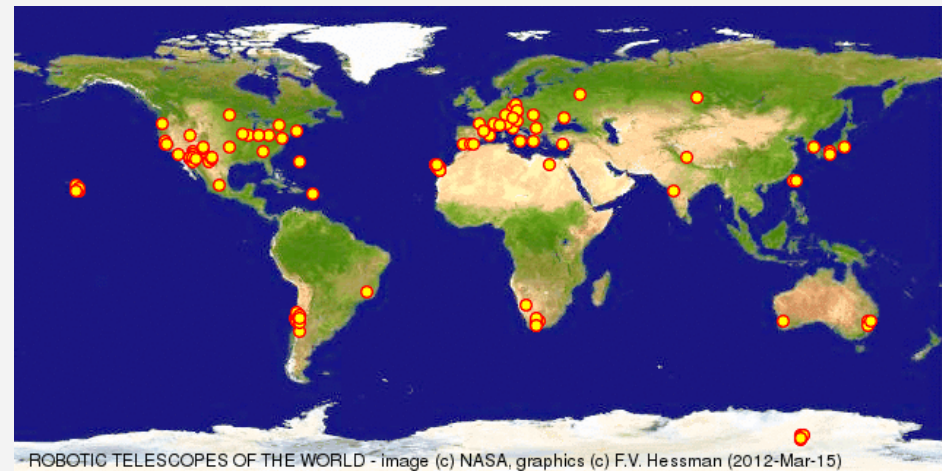
- The afterglow of GRB 970508 was the first to be observed simultaneously over almost the whole electromagnetic spectrum, several hours after the burst. In figure three spectral breaks connecting different power law segments appear clearly, at three frequencies. This behavior is fully consistent with the fireball model (more later). The complete spectrum with its breaks strongly supports the idea that GRB afterglows are powered by **synchrotron emission of electrons accelerated in a relativistic shock**.

GRB Coordinates Network (GCN)



PI: S. Barthelmy (NASA)

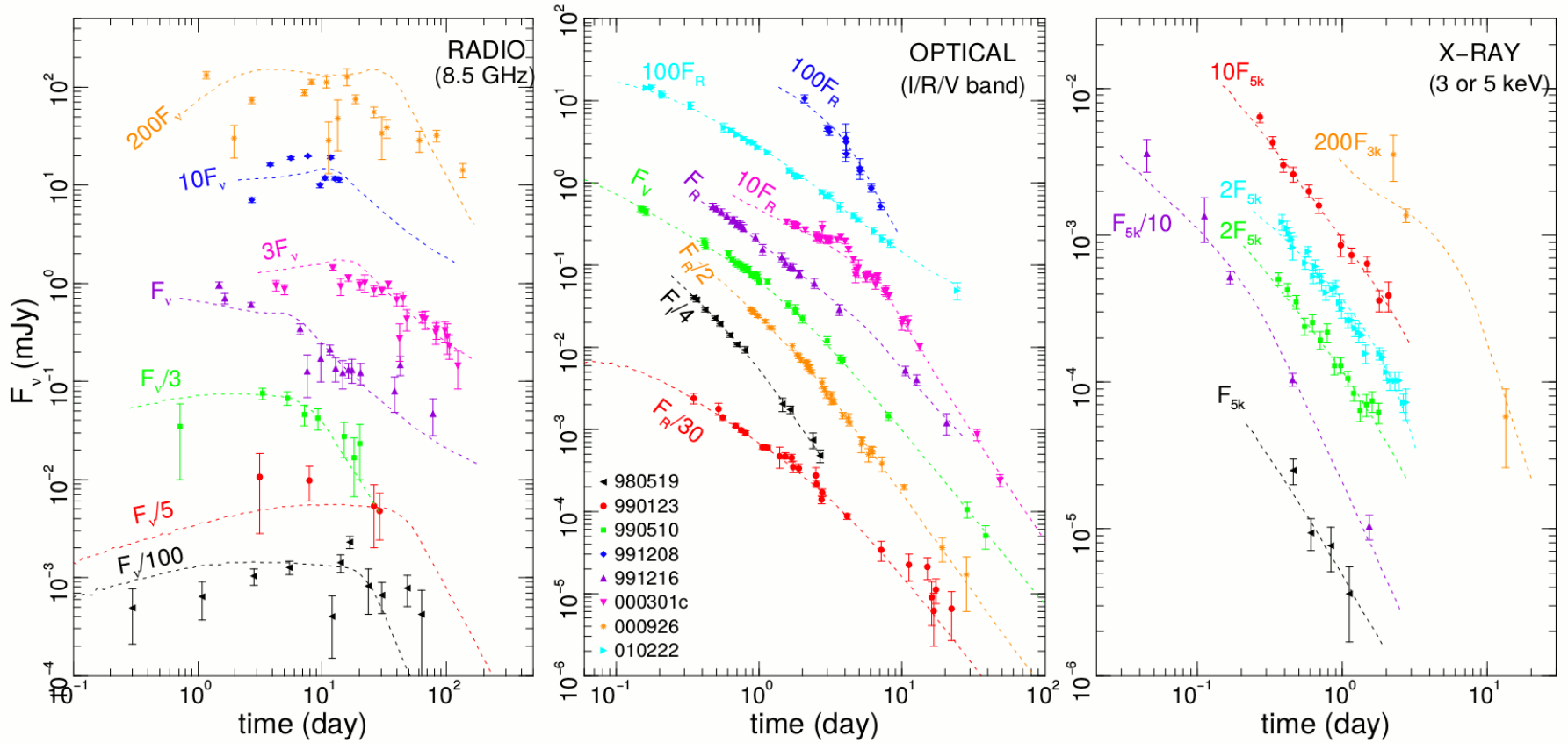
- **GCN Notices**: Alerts with real-time localisations of GRBs by various spacecraft often when the burst is not over yet are sent to the observatories e.g. ground-based robotic telescopes (e.g. BOOTES, Pi of the Sky, BART, LOTIS, MASTER, ROTSE, TAROT, ...).
- **BACODINE Notices** (obsolete): Real-time data transmission of BATSE for earliest robotic telescopes.



ROBOTIC TELESCOPES OF THE WORLD - image (c) NASA, graphics (c) F.V. Hessman (2012-Mar-15)

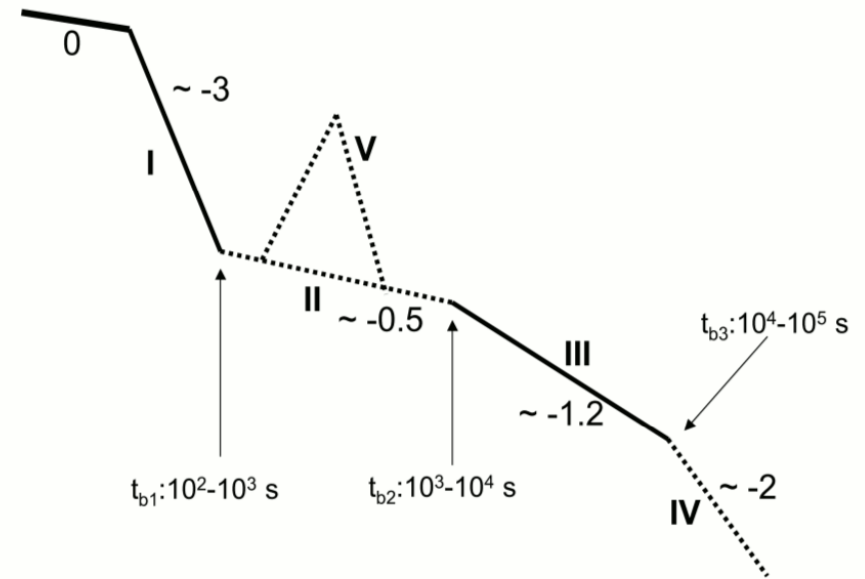
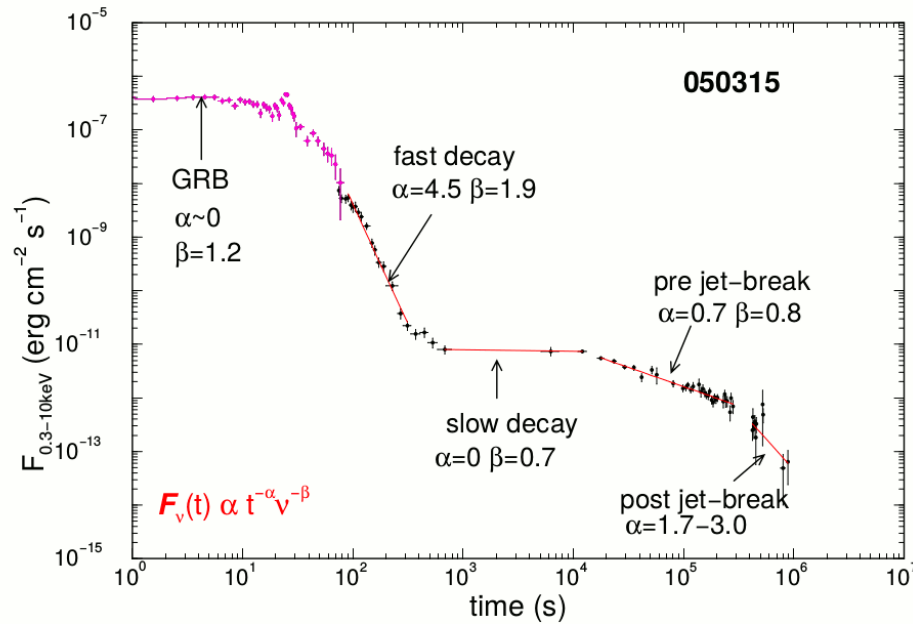
GRB Afterglows

- In most cases the afterglow light curve cannot be described as one power-law but as a sequence of power-laws with different slopes and separated by one or more breaks.



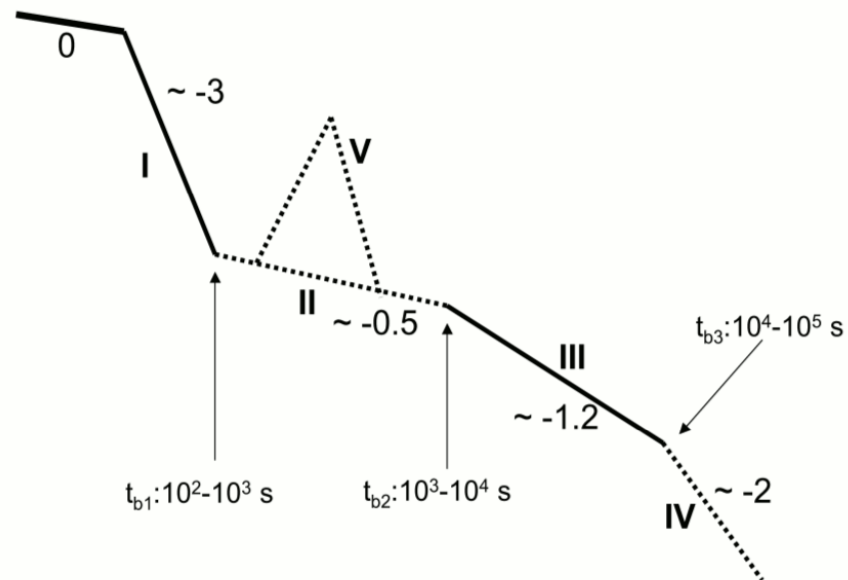
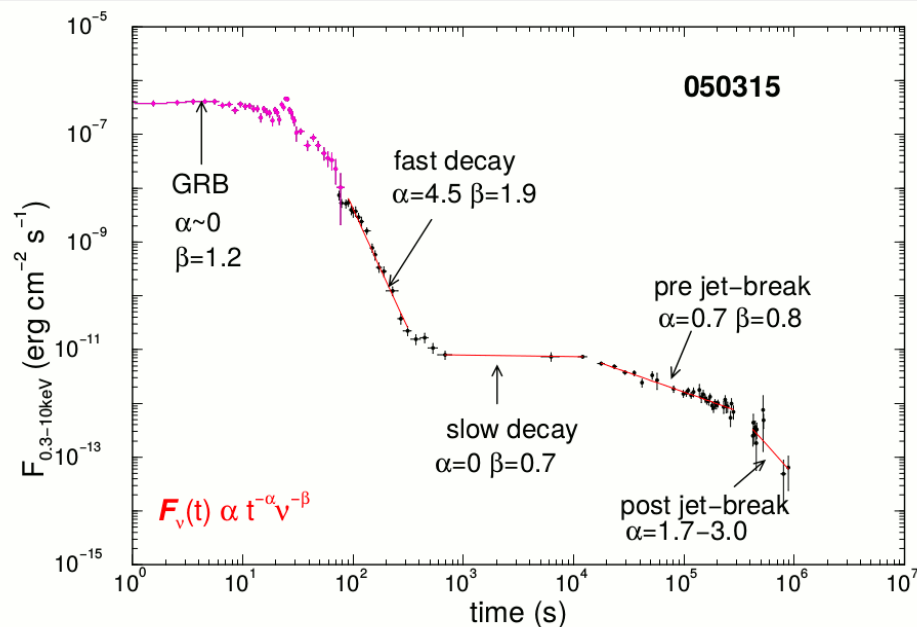
(Panaitescu & Kumar 2001)

A Typical X-ray Afterglow Development



Left panel: Phases of the afterglow of GRB 050315. This GRB provides a good illustration of the typical times and properties of each phase. Magenta points denote the 15 – 150 keV Swift BAT measurements of the prompt emission. Data are extended to the 0.3 – 10 keV Swift XRT measurements (black points). Red lines represent the fits of each phase. The characteristic values of α (the temporal decay index) and β (the spectral index) of each phase are also indicated (Credit: Panaitescu 2006). *Right panel:* A cartoon of a typical X-ray afterglow based on the Swift XRT data. Phase 0 denotes the prompt emission, I denotes the prompt decay phase, II is the shallow phase with V a possible X-ray flare (a discovery of the Swift satellite). Phase III was already known from the BeppoSAX time with a possible break leading to phase IV (Credit: Zhang et al. 2006).

A Typical X-ray Afterglow Development



#	Phase	Start time	Decay	≈ freq
I	Steep decline	$10-10^2$	$\gtrsim 3$	50%
II	Shallow slope	$100 - 1000$	0.5	60%
III	Classical afterglow	$10^3 - 10^4$	1.3	80%
IV	Jet break – late phase	$10^5- 10^6$	2.3	20%
V	Flares (X-ray)	$10^2 - 10^4$	N/A	50%

Association with SNe

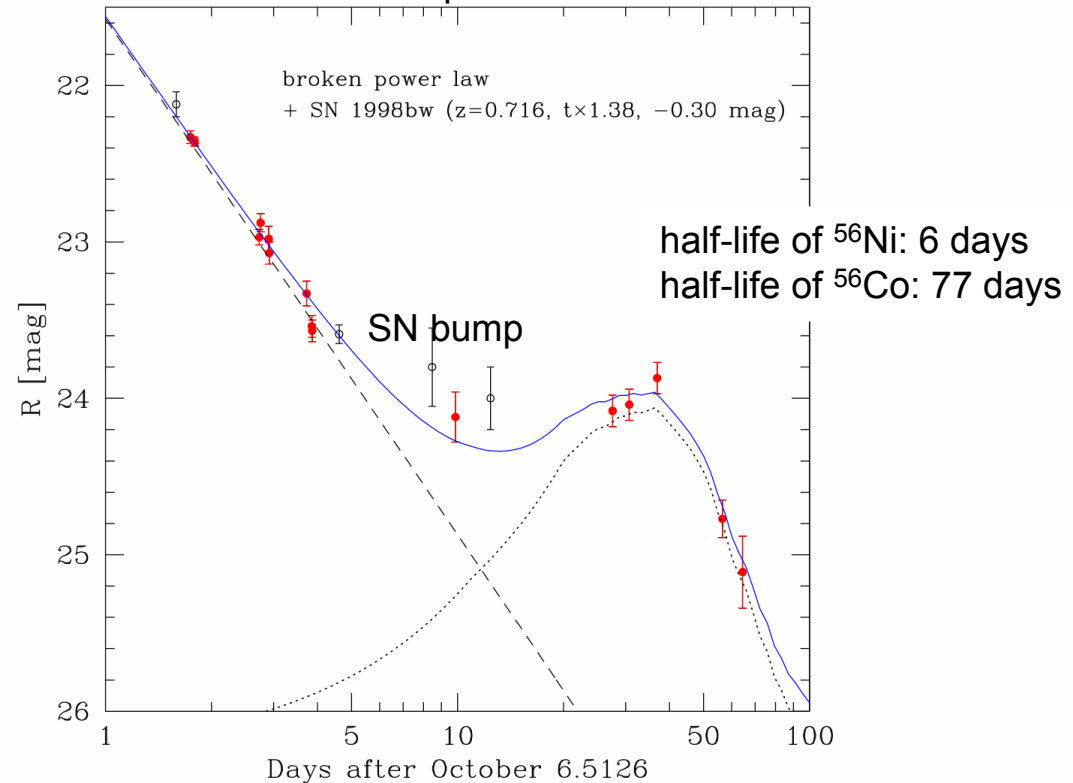
Long GRBs and SNe Ic Connection

- The first GRB/SN association was GRB 980425 / SN 1998bw, nearby and very bright type Ic supernova (core-collapse, no He lines). The explosion was unusually energetic, more than 10 times that of an ordinary supernova. GRB 980425 is the closest burst recorded to date with redshift $z = 0.0085$, i.e. only 37 Mpc.
- Some (not all) long-duration bursts are associated with core-collapse supernovae Ic.



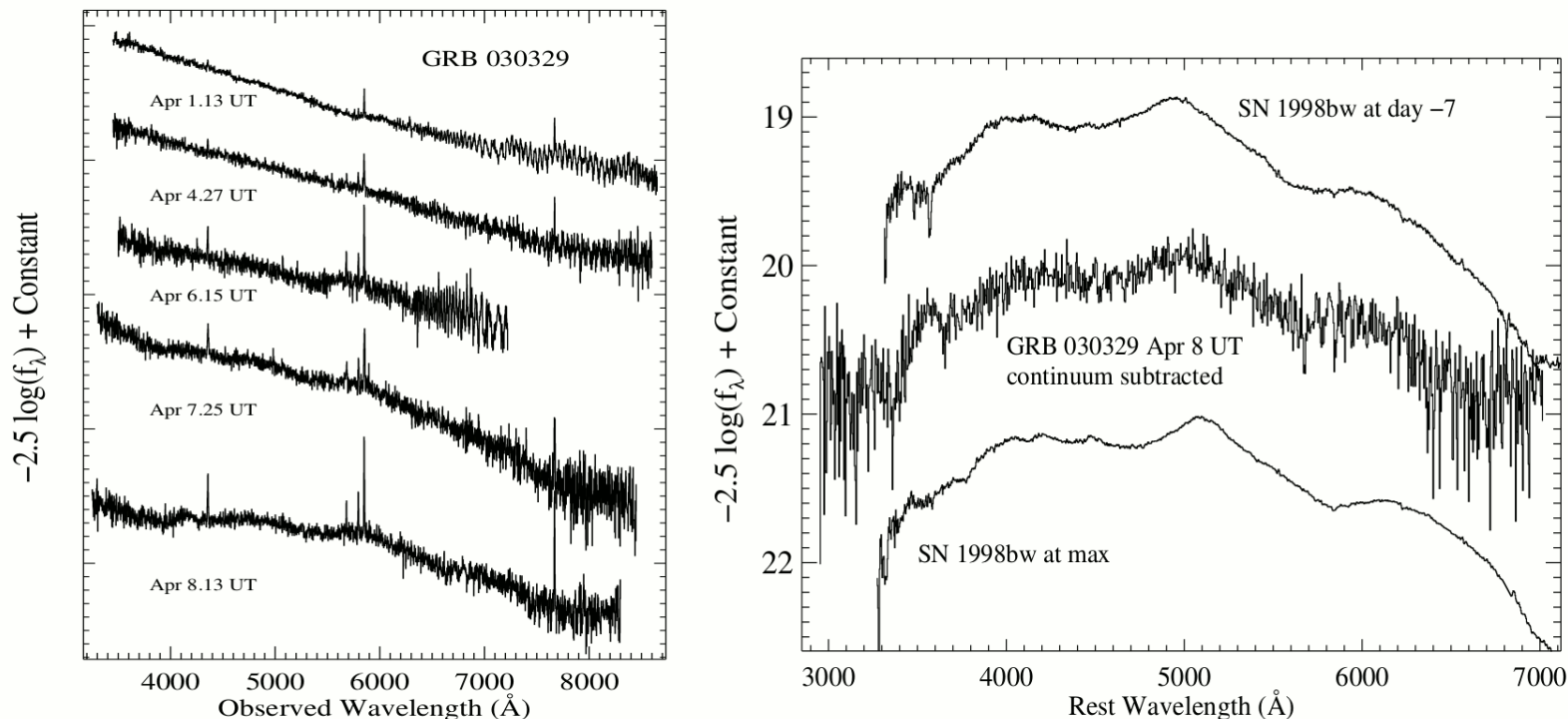
GRB 980425 / SN 1998bw

Another example: GRB 041006



The R band light curve of the afterglow of GRB 041006 (red and opened circles denote data from different authors). The power-law decay with a slope of -1.3 is shown by the dashed line. A supernova SN 1998bw light curve extended by a factor 1.38 is indicated by the dotted curve. The solid curve denotes the combination of both components. The supernova bump, powered by the radioactive decay $^{56}\text{Ni} \rightarrow ^{56}\text{Co} \rightarrow ^{56}\text{Fe}$ (by K-capture), is clearly evident (Credit: Stanek et al. 2005).

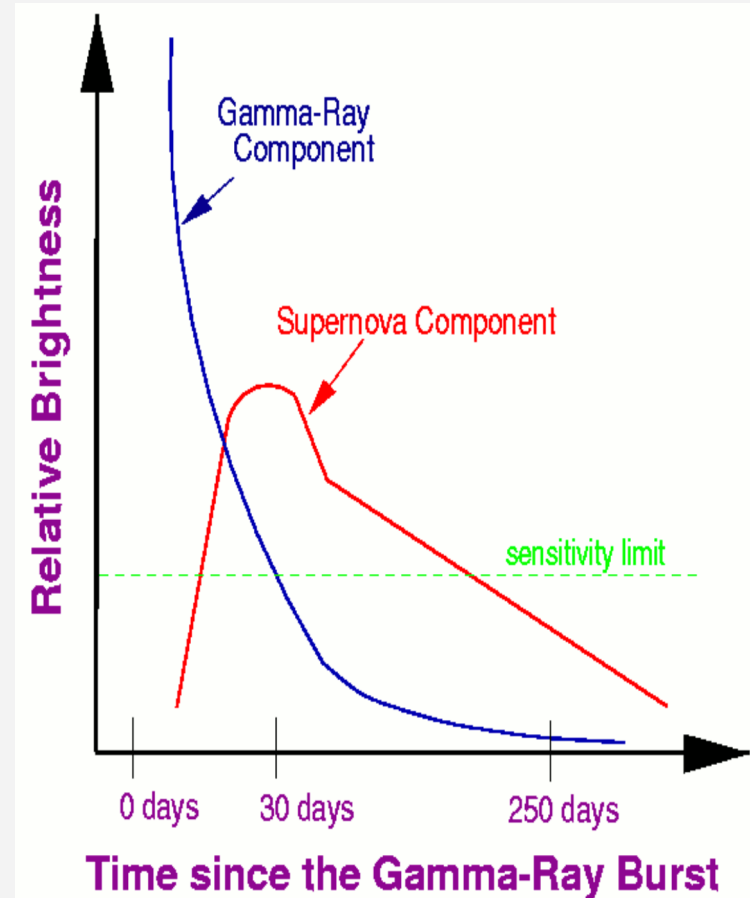
The Spectroscopic Confirmation of GRB/SN Connection



Left panel: Evolution of the GRB 030329/SN 2003dh spectrum, from April 1.13 UT (2.64 days after the burst) to April 8.13 UT (9.64 days after the burst). The early spectra consist of a power-law continuum with narrow emission lines originating from HII regions in the host galaxy at a redshift of $z \approx 0.168$. Spectra taken at later times, after April 5, show a development of broad peaks in the spectra characteristic of a supernova.

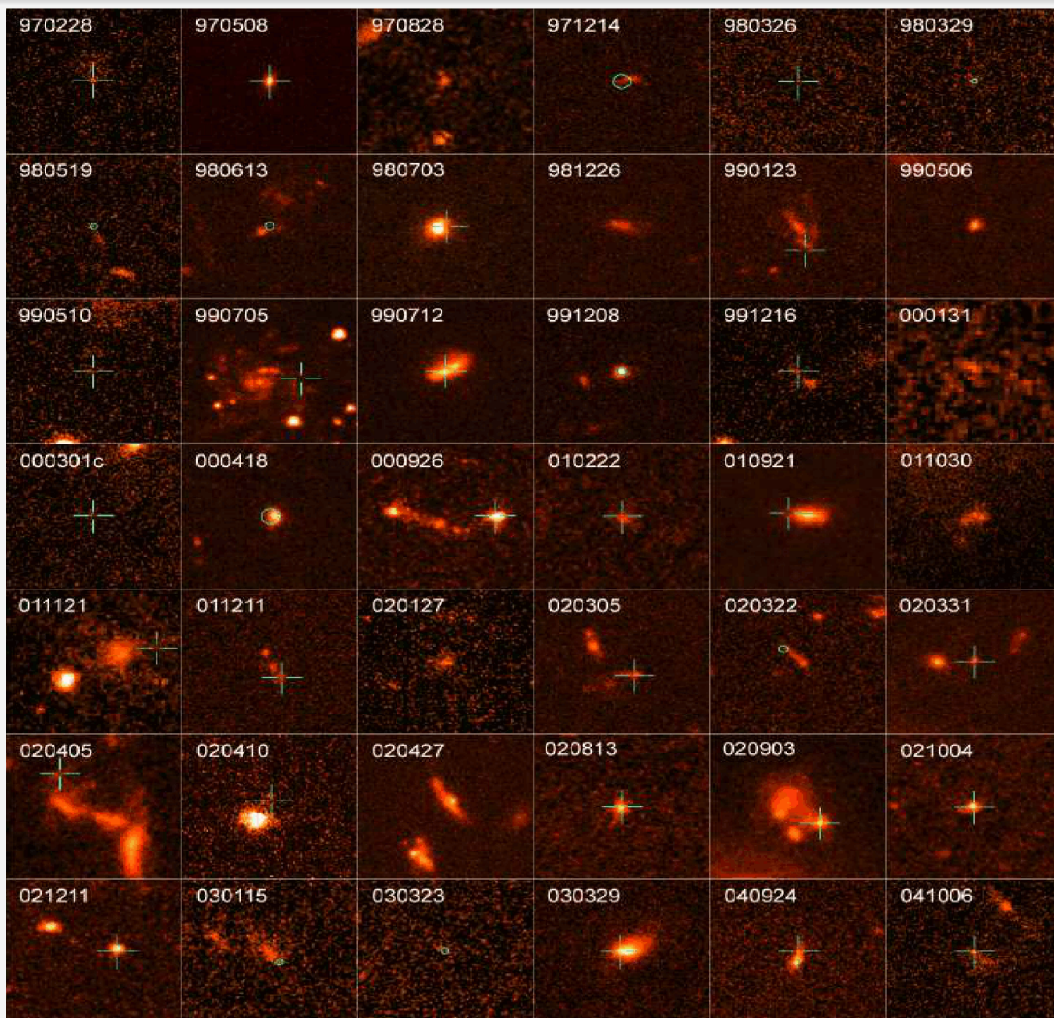
Right panel: The spectrum measured on April 8 with continuum subtracted. The residual spectrum shows broad bumps at approximately 5000 and 4200 \AA (rest frame), which is similar to the spectrum of the peculiar Type Ic SN 1998bw a week before maximum light. (Credit: Stanek et al. 2003).

- SN light much fainter than average GRB afterglow
- Need nearby GRBs to see it
- Need faint afterglow to see it



Credit: in't Zand

GRB Host Galaxies



- A sample of GRB host galaxies imaged by HST. The positions of bursts are indicated by a green mark (Fruchter et al. 2006).

For long GRBs ($T_{90} > \sim 2s$):

- Irregularly shaped and low metallicity.
- Consistent with abundant presence of massive stars.
- Increased star formation rates (indicated by OII line).
- GRBs sit on brightest parts of host galaxies.
- Young stellar population.
- Association with core-collapse type Ic SNe.

For short GRBs ($T_{90} < \sim 2s$):

- Mix of early and late type galaxies.
- Kicks/migration from their birth sites. → offset between GRB and host
- No supernova associated.
- Association with kilonova (macronova).
- merging of compact objects (NS-NS or NS-BH).

- GRB 990123
- GHostS (GRB Host Studies) <http://www.grbhosts.org>

Redshift Measurements

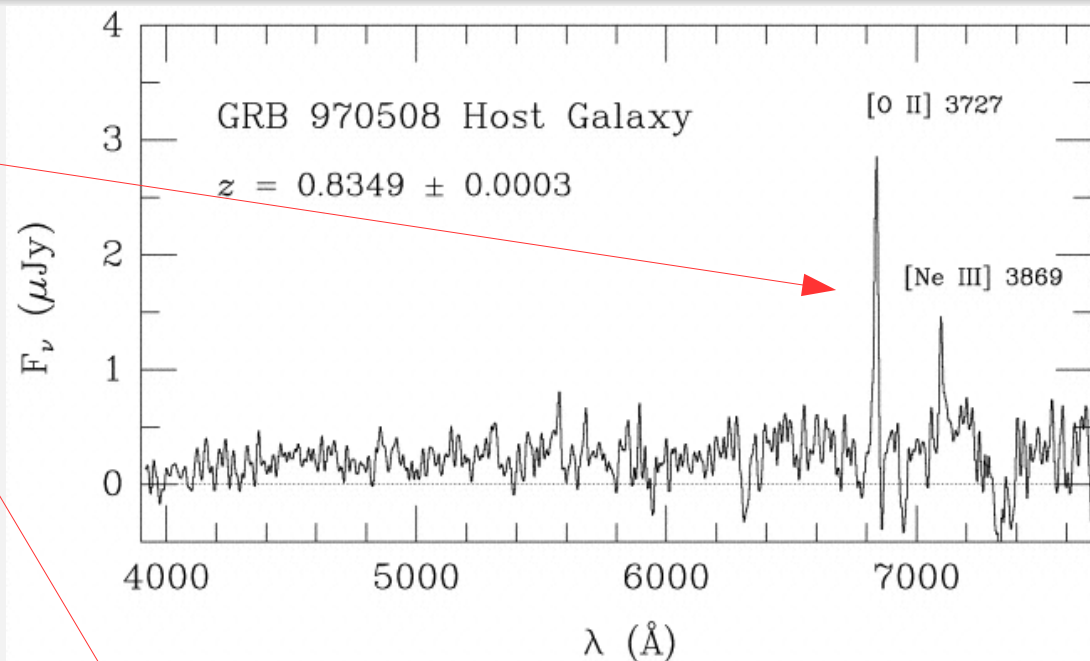
Spectroscopic Redshift Determination

Spectroscopic redshift either through:

- **Emission features in the spectrum of the host galaxy.**

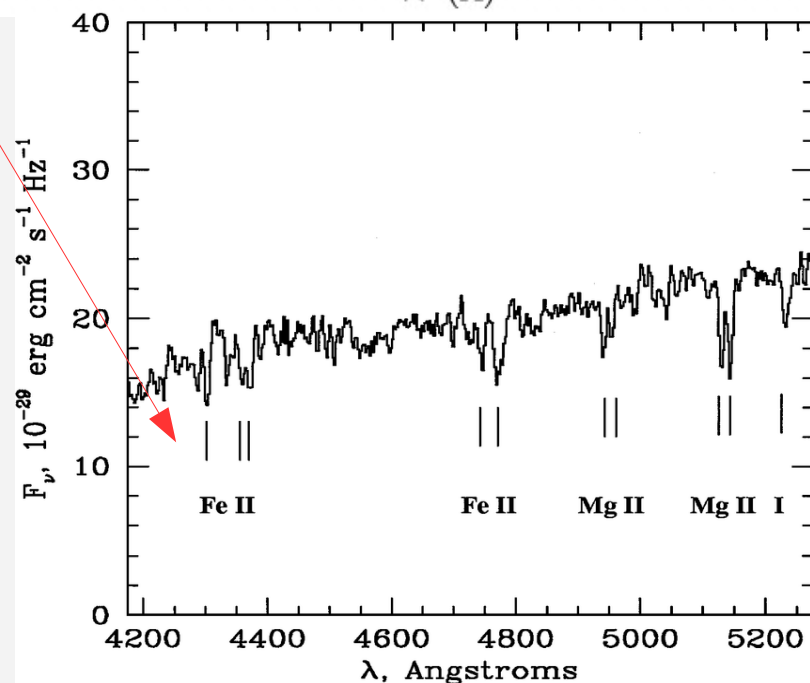
or

- **Absorption features in the afterglow spectrum.**



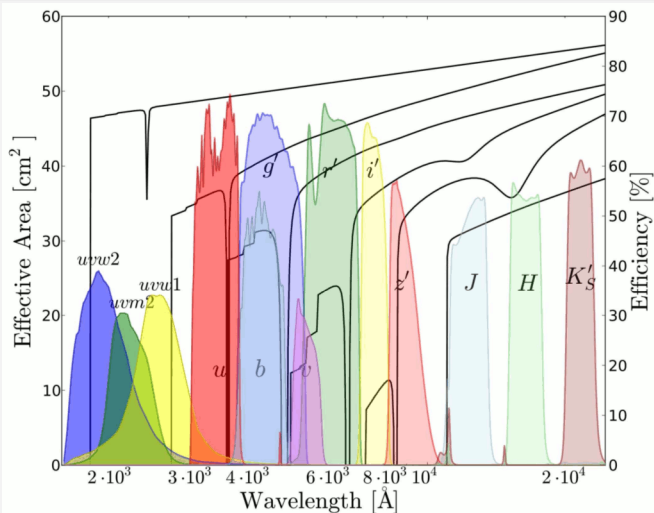
Top: The spectrum of the host galaxy showing O II and Ne III emission lines at redshift $z = 0.835$.

Bottom: The spectrum of the optical afterglow of GRB 970508 showing Fe II and Mg II absorption lines at the same redshift (Metzger et al. 1997, Bloom et al. 1998).

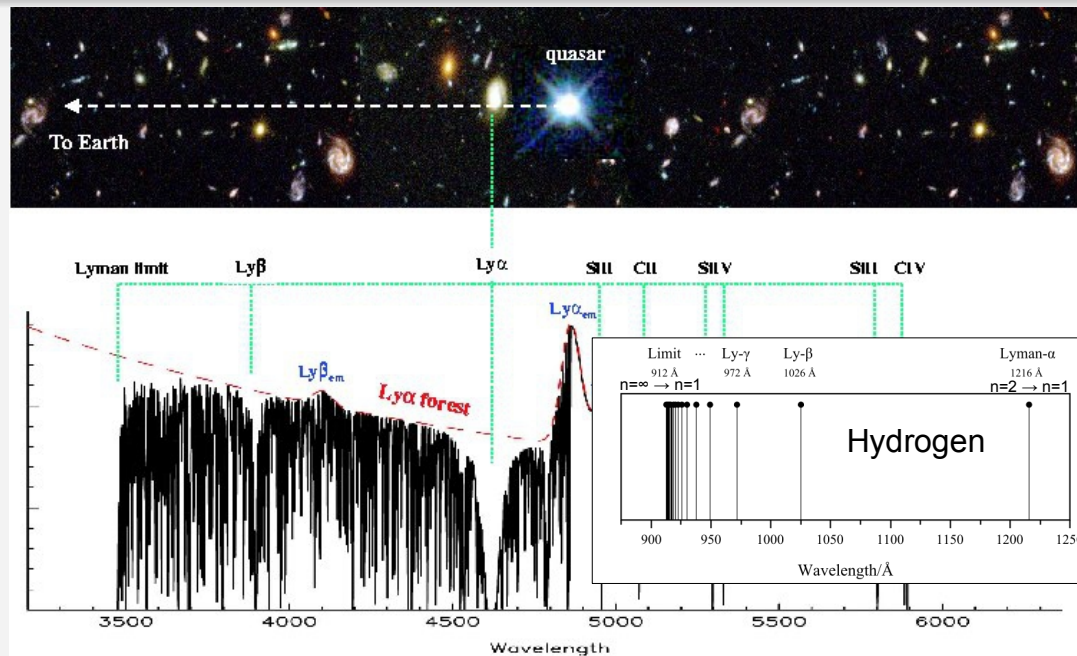


→ $E_{\text{iso}} = 7 \times 10^{51} \text{ erg}$

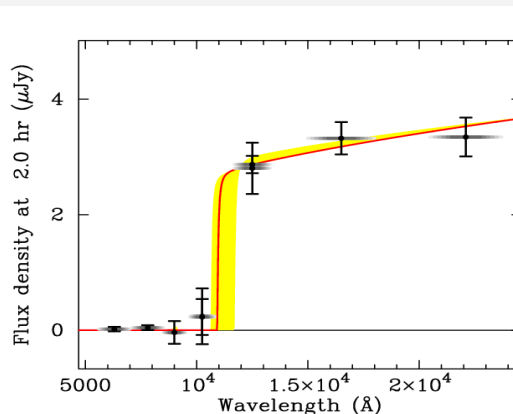
Photometric Redshift Determination



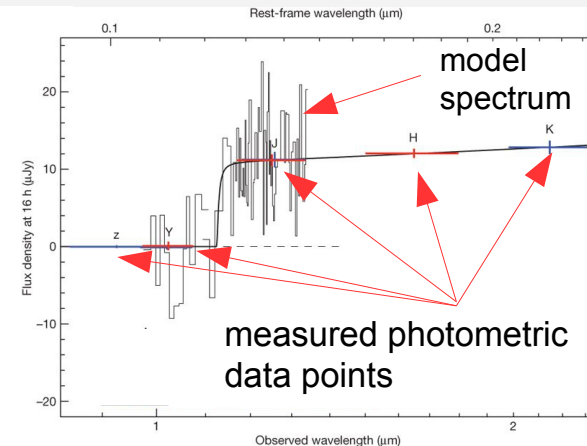
Swift/UVOT and GROND telescope filters (Krühler et al. 2011)



- Photometric redshift measurement requires high-quality photometry over a large wavelength range.
- Two prominent signatures, the Ly- α and Lyman-limit allow redshift determination by fitting a model spectrum.

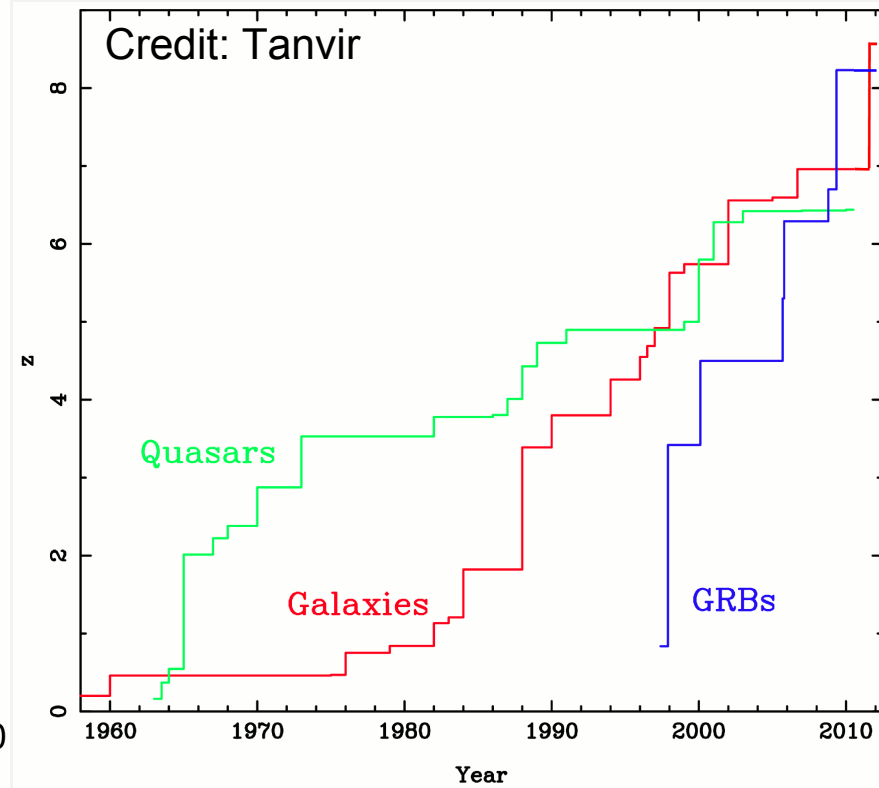
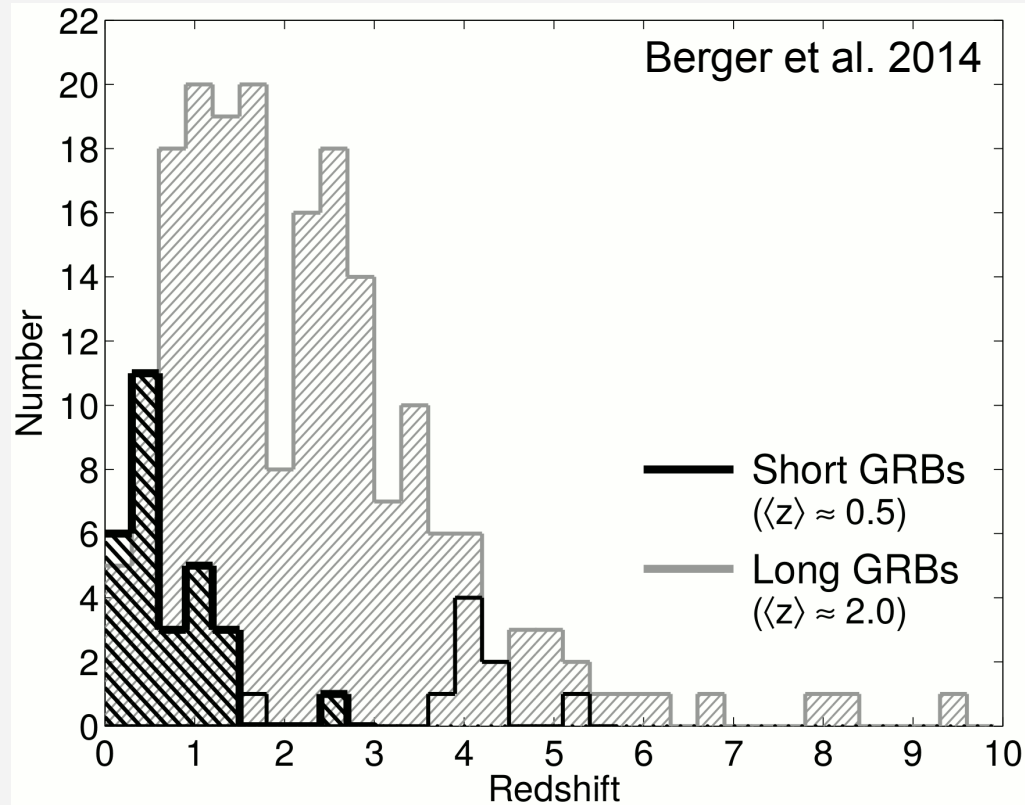


Spectrum of afterglow of GRB 120923A with best fit to Lyman- α limit at $z = 8.5$. (Tanvir et al. 2013).



GRB 090423 afterglow spectrum, redshift of $z = 8.23$ (Tanvir et al. 2009).

Redshift Distribution



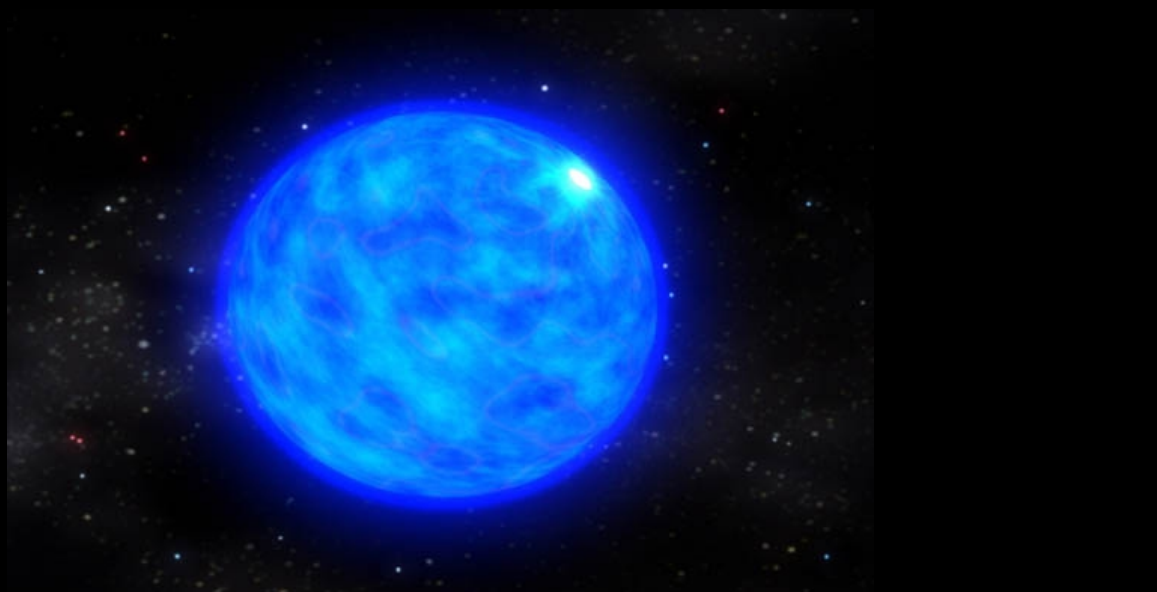
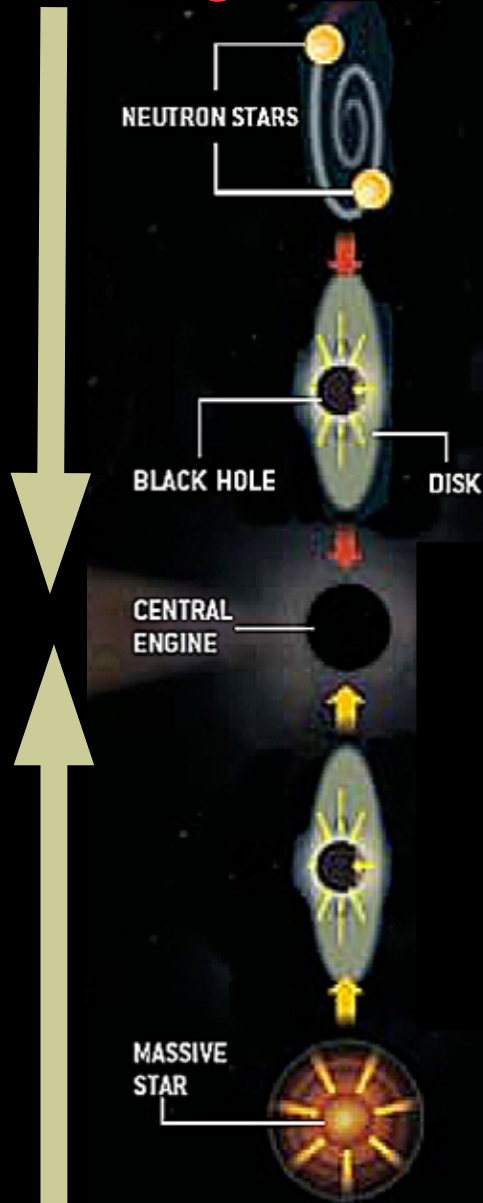
Least distant observed: $z = 0.0085$ (GRB 980425)

Most distant observed: $z = 9.4$ (GRB 090429B)

Relativistic Fireball Model

Formation of GRB: Two Scenarios and Fireball Model

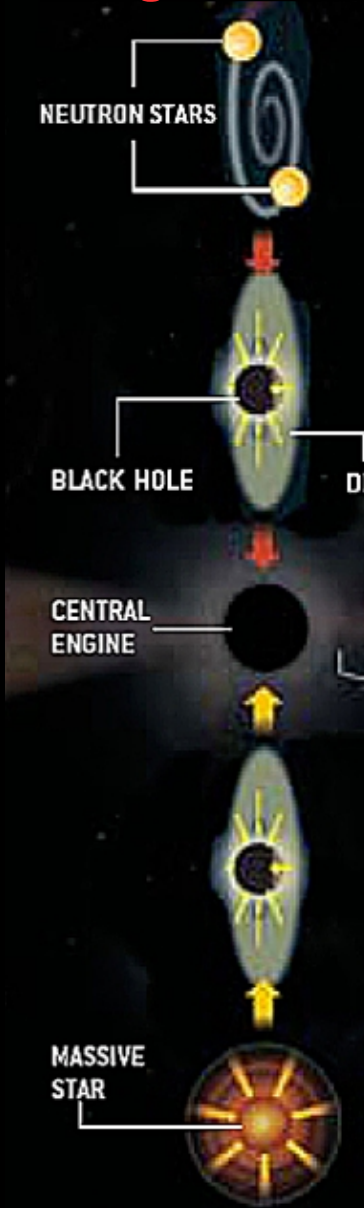
Merger scenario



Hypernova scenario

Fireball Model

Merger scenario



First introduced by P. Mészáros & M. Rees 1992, 1994
(also Paczynski & Rhoads 1993)



GAMMA-RAY EMISSION

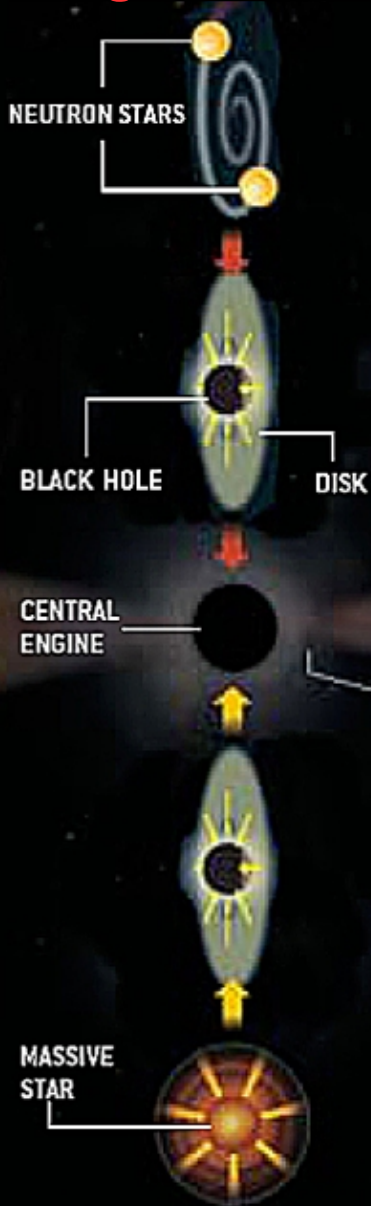
External shock wave



Hypernova scenario

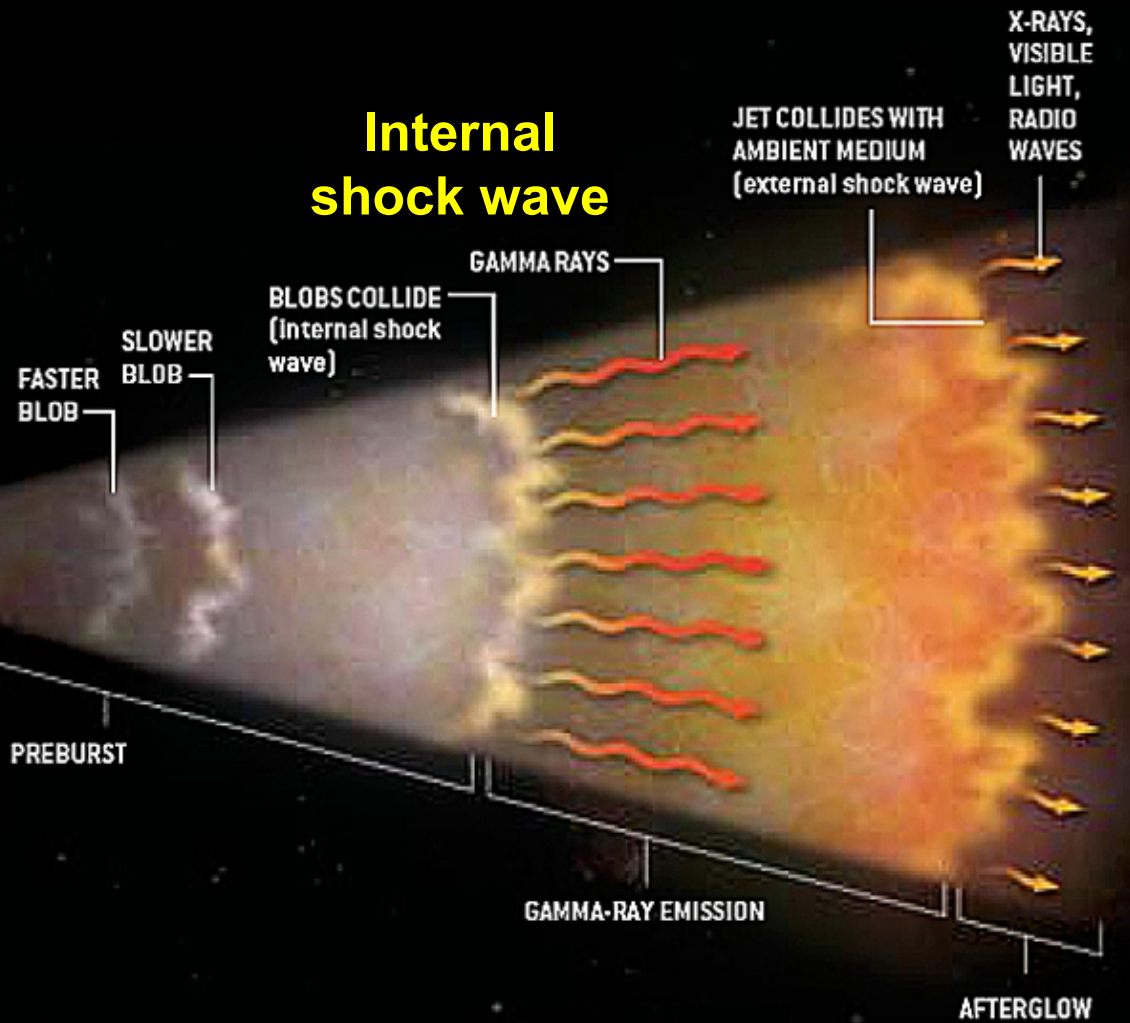
Fireball Model

Merger scenario



External shock wave

Internal shock wave



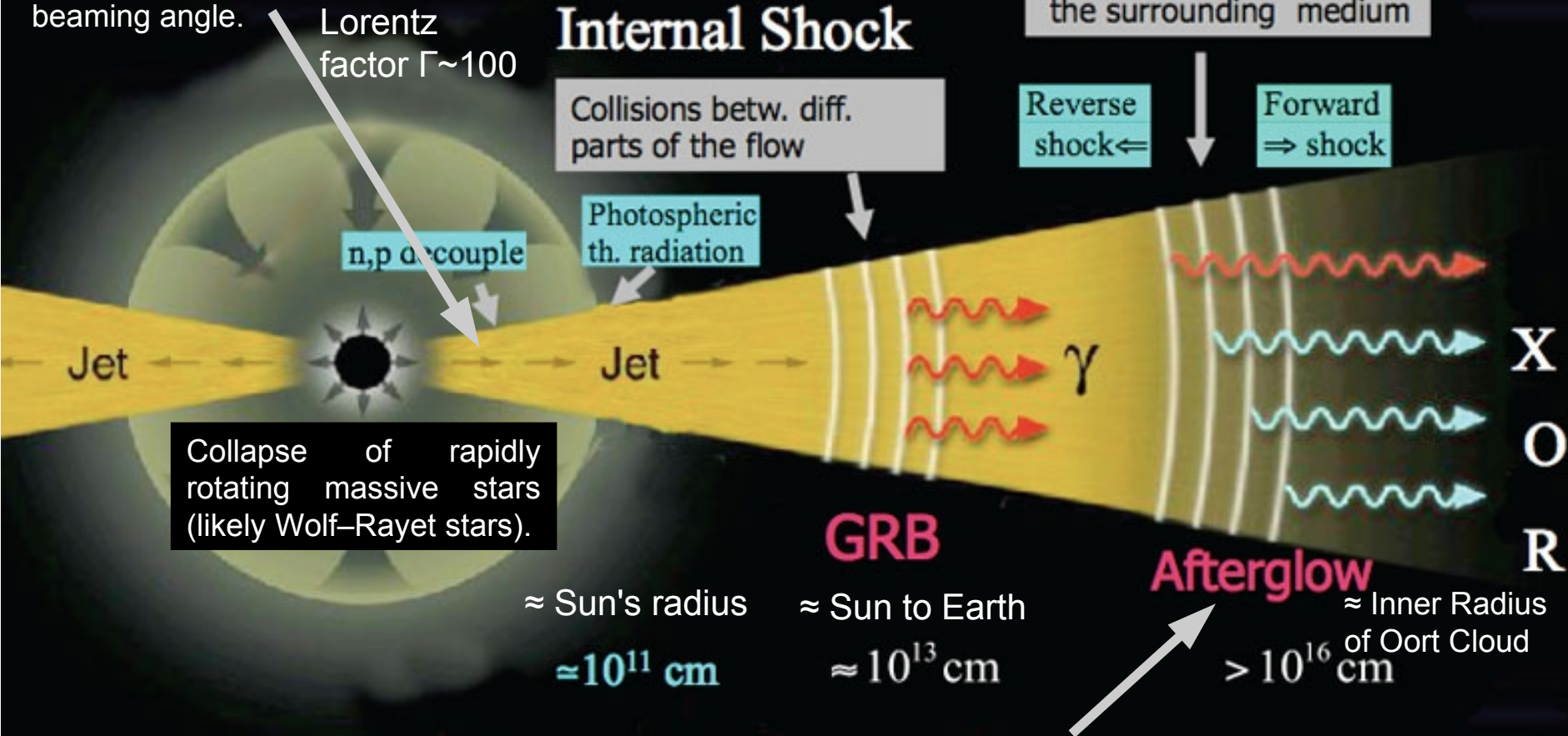
Hypernova scenario

Fireball Model and Collapse of Massive Star as Progenitor

- Long-duration GRBs: equivalent isotropic energy up to $>10^{54}$ erg

Phase of acceleration: the thermal or magnetic energy is converted into kinetic energy of baryons within the ejecta that creates an ultrarelativistic jet with a certain beaming angle.

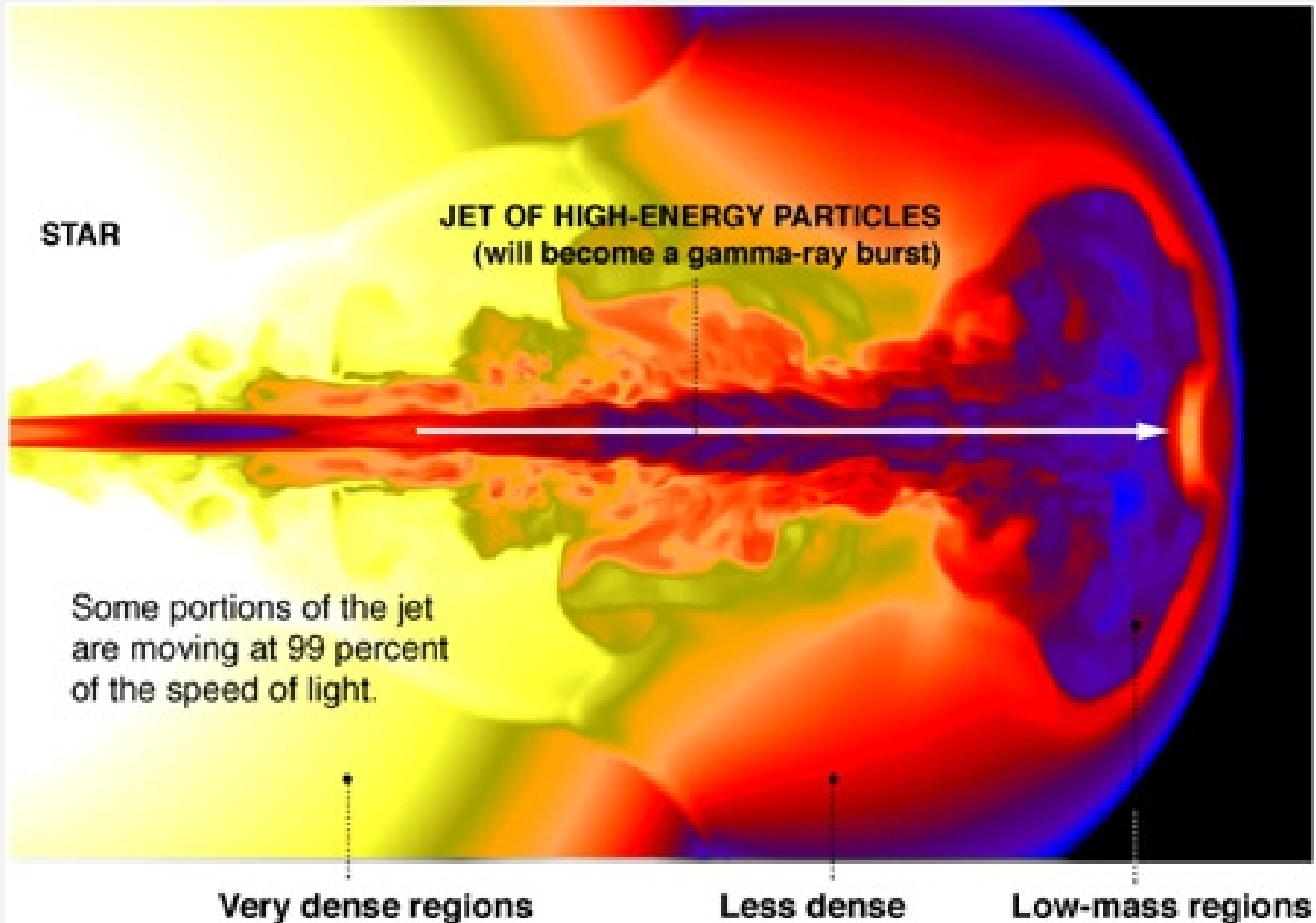
Lorentz factor $\Gamma \sim 100$



The ultrarelativistic jet is decelerated by the swept-up circumburst medium. The optical afterglow is released via synchrotron emission from external shocks, where the kinetic particle energy is transformed into radiation.

Simulation of the GRB Jet

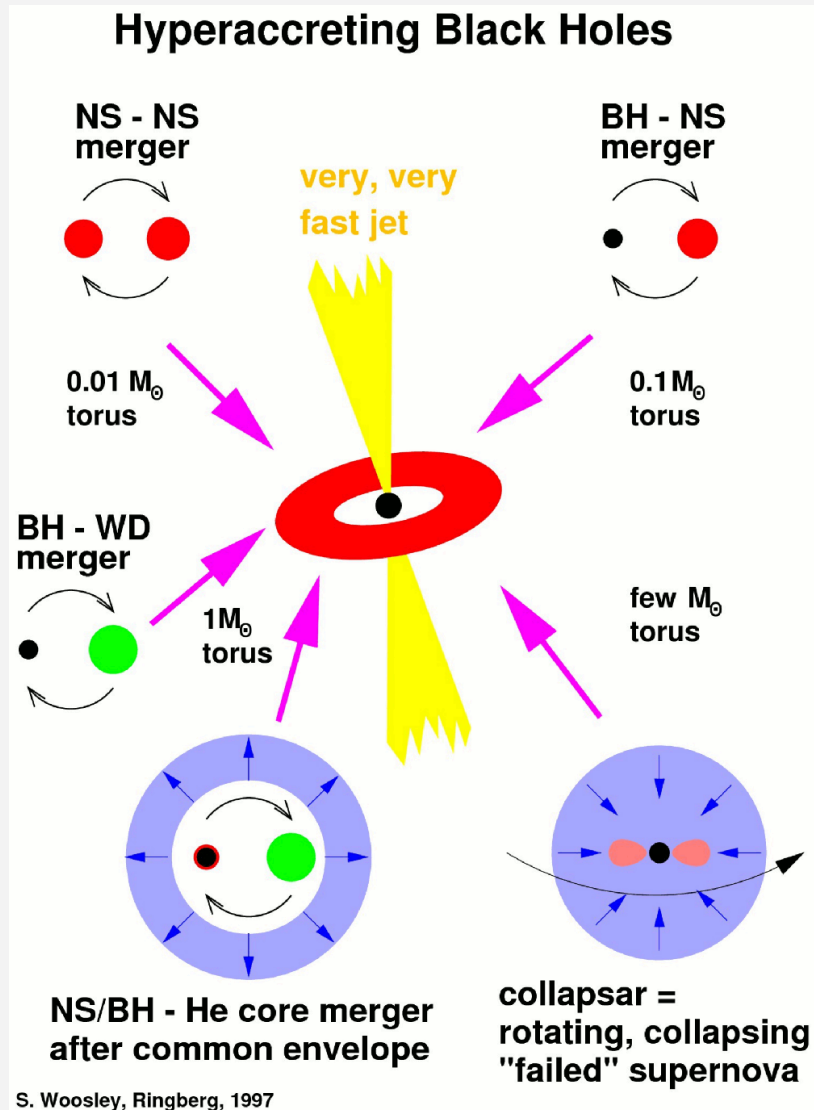
This relativistic hydrodynamic simulation shows the distribution of relativistic particles (moving near light speed) in the jet as it breaks out of the star. Yellow and orange are very high energy and will ultimately make a gamma-ray burst, but only for an observer looking along the jet (\pm about 5 degrees). Note also the presence of some small amount of energy in mildly relativistic matter (blue) at larger angles off the jet. These will produce X-ray flashes that may be much more frequently seen.



Credit: W. Zhang and S. Woosley

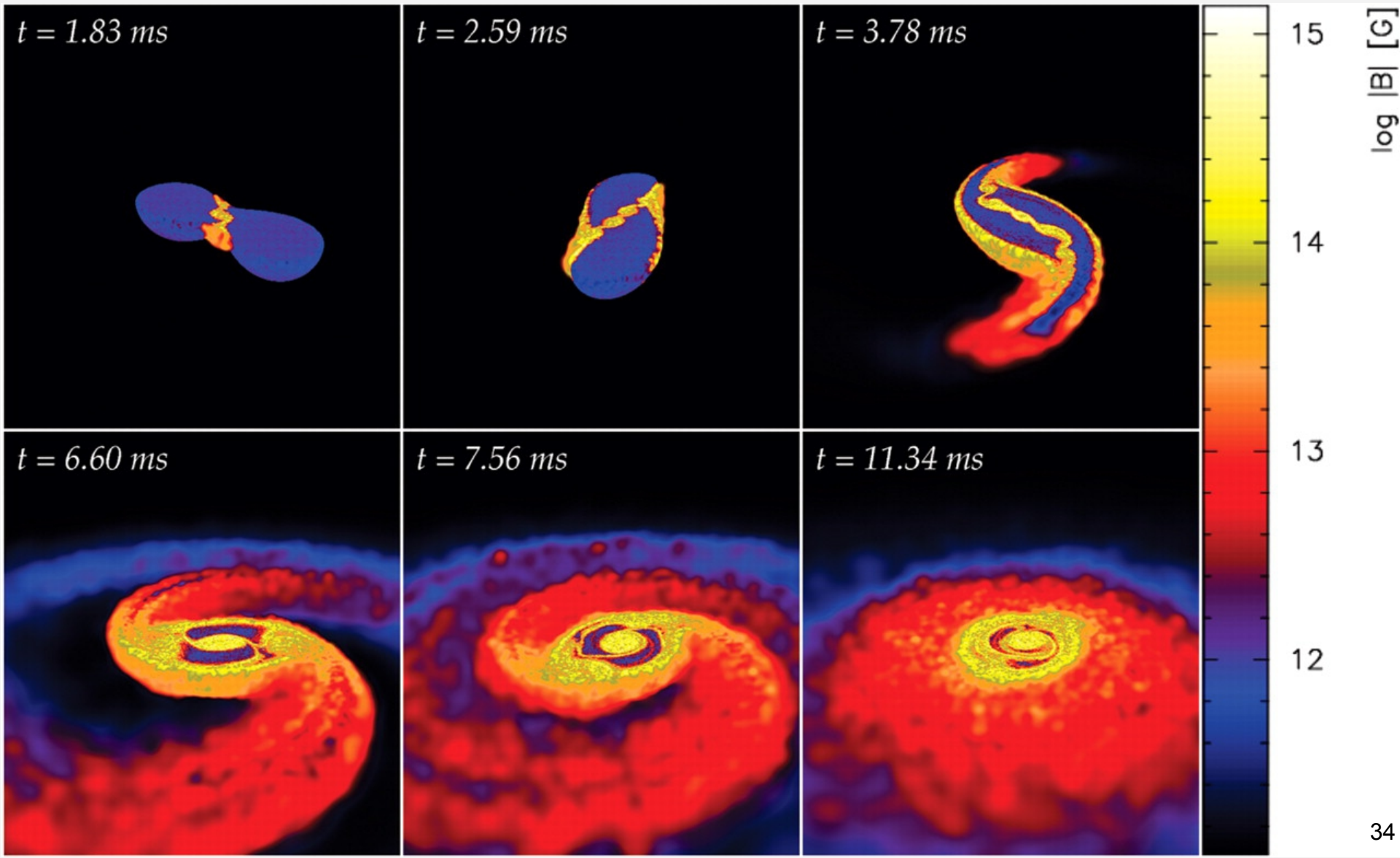
Merger of Compact Objects as Progenitor

- Short-duration GRBs: equivalent isotropic energy up 10^{51} - 10^{52} erg
- Introduced by Paczyński (1986) and Eichler et al. (1989).



Simulation of Merger two Neutron Stars

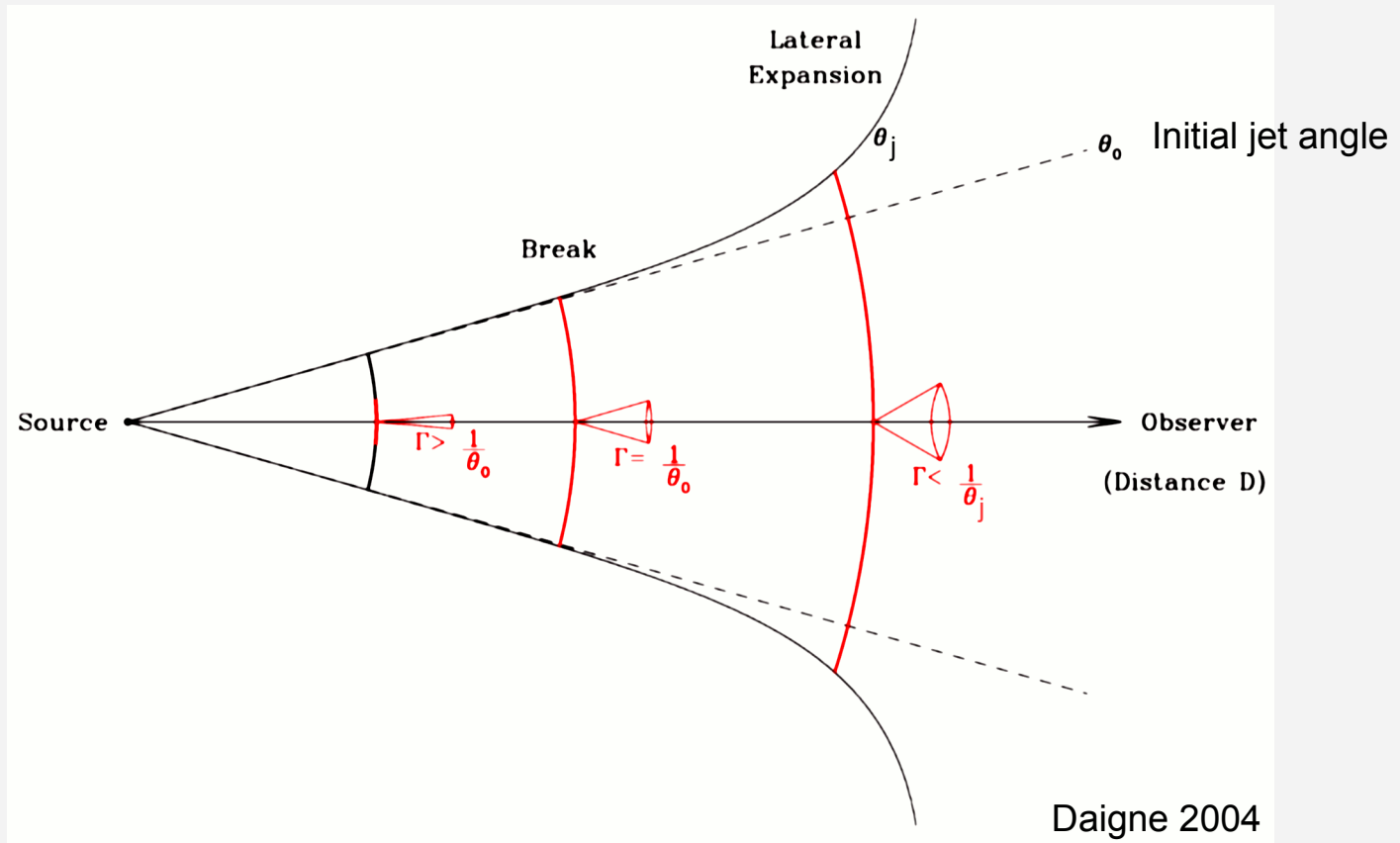
- A magnetohydrodynamic simulation of a merger of two magnetized NS. Colors indicate $\log(B)$, maximal magnetic field strength reaches 10^{15} G. The left to right dimension of the panels is ~ 140 km (Price & Rosswog 2006).



Multi-Wavelength Afterglow Observations and Jet Breaks

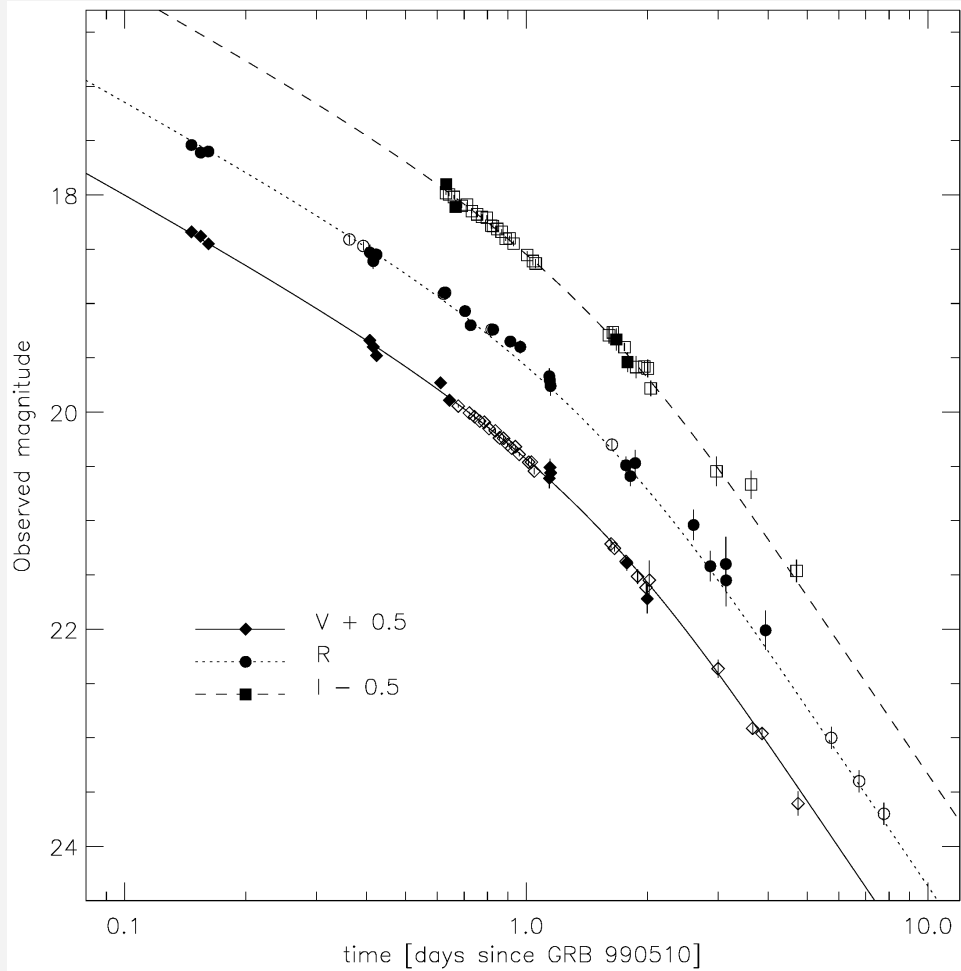
Achromatic Break Due to Jet

- Achromatic (not depending on wavelength) break happens if the relativistic beaming angle (relativistic aberration) of the emitted photons $\theta_r \sim \Gamma^{-1}$ increases over the jet angle θ_j of the ejecta.
- Time of break constrains the jet angle θ_j .

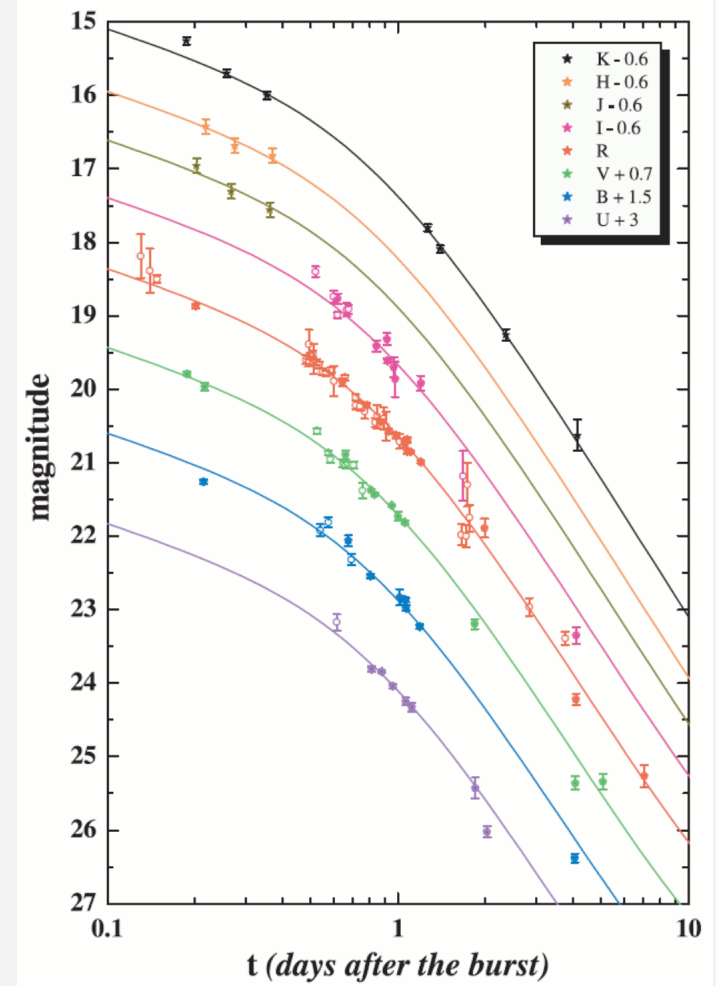


Problem: only minority of multi-wavelength GRB afterglows shows clear break.

Observed Achromatic Jet Breaks

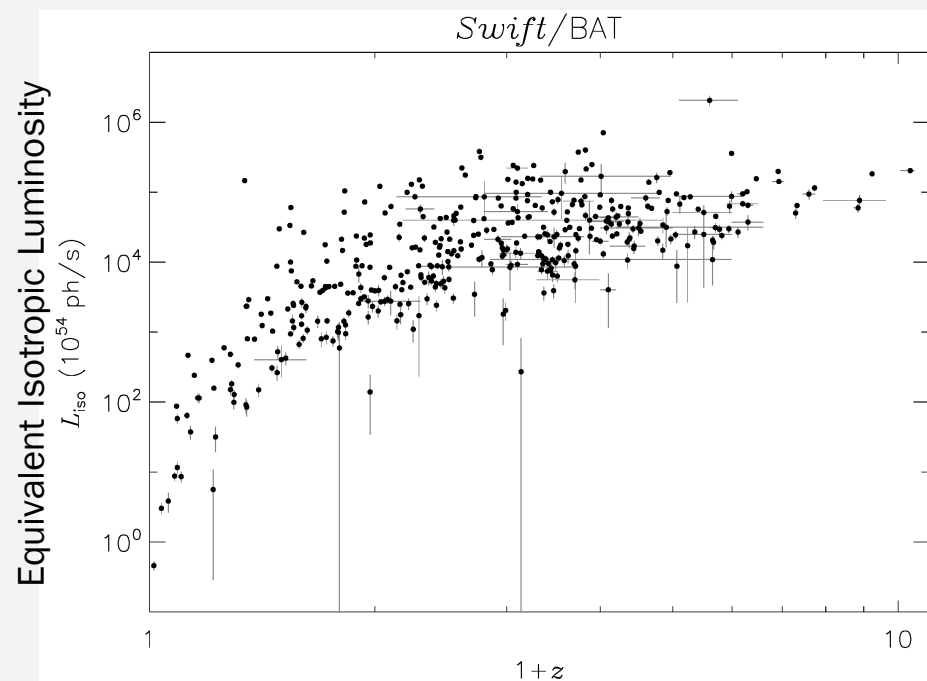
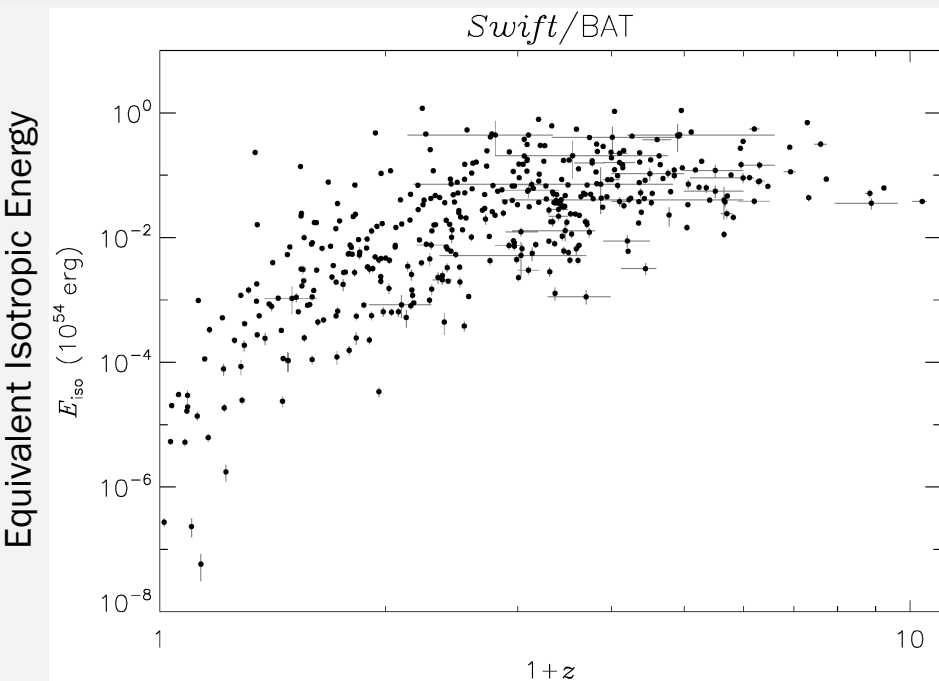


Light curves of the optical afterglow of GRB 990510, measured at different wavelengths, clearly showing an achromatic break (Harrison et al. 1999).



GRB 030326

Burst Energetics



- Equivalent isotropic energy and luminosity is assuming isotropic emission.
- A seeming relation, but two selection effects give such an appearance:
 - 1) There are more low-fluence bursts than high-fluence (which is why we haven't seen high-fluence ones yet in the nearby universe due to small volume covered).
 - 2) The low-fluence bursts at high redshifts are below detection threshold.

Burst Energetics

- As most GRBs are probably collimated with typical opening angles between 1° and 30° , the true released energy in gamma rays is around 10^{50} to 10^{52} ergs.

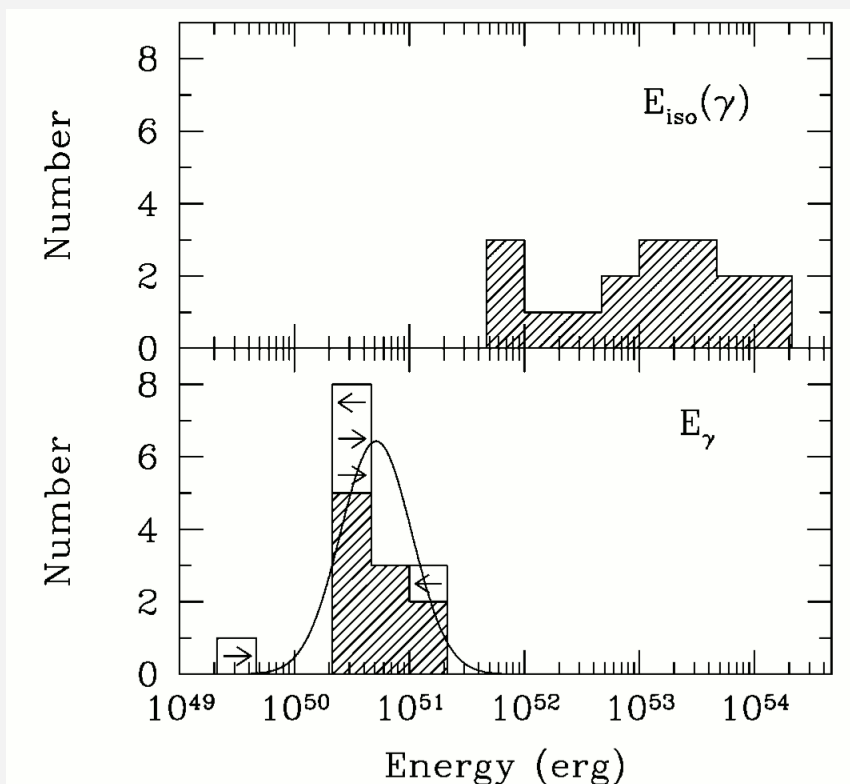
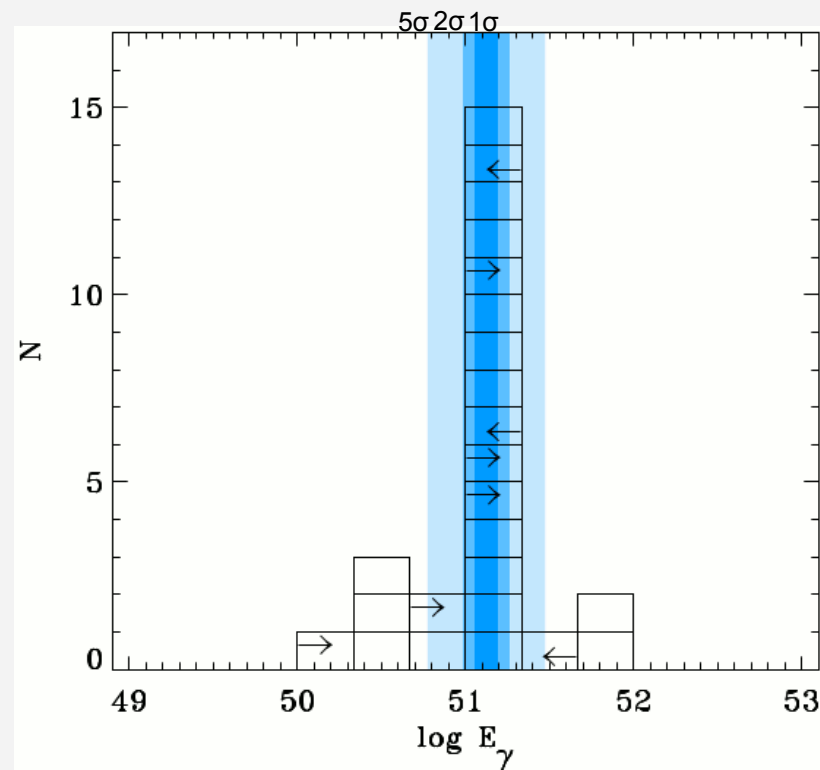


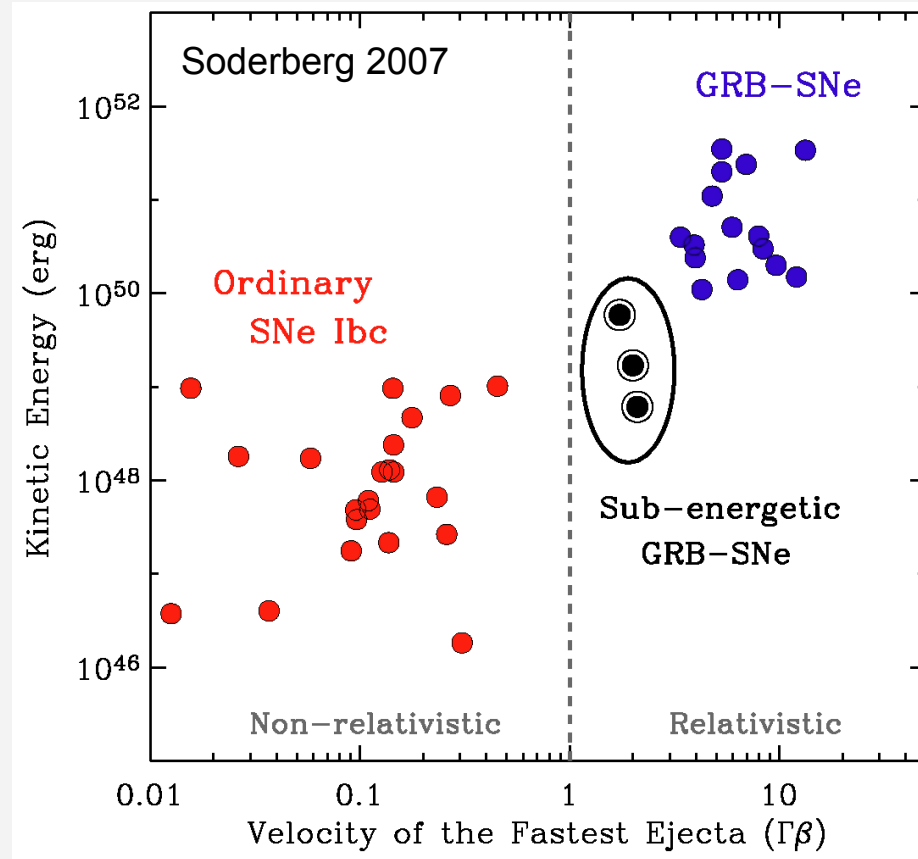
FIG. 2.—Distribution of the apparent isotropic GRB energy of GRBs with known redshifts (*top panel*) vs. the geometry-corrected energy for those GRBs whose afterglows exhibit the signature of a nonisotropic outflow (*bottom panel*). Arrows are plotted for five GRBs to indicate upper or lower limits to the geometry-corrected energy. (Frail et al. 2001)



Histogram of GRB energies E_γ showing a narrow distribution about 10^{51} erg (Bloom et al. 2003).

Burst Energetics

- The kinetic energy of GRB ejecta is similar order: about 10^{51} erg.



- Not all SN Ib/c produce long GRBs.